Enhancing En-route Electric Vehicle Charging Services with AI Integration: A Collaborative Fog-based Strategy for Optimizing Sustainable Transportation

by

Samira Hosseini

A thesis submitted to the Lakehead University in partial fulfillment of the requirement for the degree of Master of Science (MSC) in Electrical and Computer Engineering

Lakehead University, Thunder Bay, Ontario, Canada

Examining Committee Membership

The following served on the Examining Committee for this thesis.

Supervisor(s): Dr. Abdulsalam Yassine,
Department of Software Engineering, Lakehead University, Thunder Bay

Examiner(s): Dr. Yong Deng, Dr. Thangarian Akilan

Author's Declaration

I hereby declare that I am the sole author of this thesis. This is a true copy of the thesis, including any required final revisions, as accepted by my examiners.

I understand that my thesis may be made electronically available to the public.

Signed: _____

Date: _____

Abstract

In the emergence of greener transportation, Electric Vehicles (EVs) play an important role, expected to outnumber conventional vehicles in the near future. However, the installation of Fixed Charging Stations (FCSs) is not keeping up with the increased demand, especially outside urban centers. Such a challenge is prohibiting many users from owning EVs because of range anxiety. This thesis proposes a novel cooperative mechanism where EVs can access charging services such as Vehicle-to-Vehicle (V2V) charging schemes, private smart Home Charging Station (HCS), or Mobile Charging Station (MCS) to complement existing FCS services in certain regions. To this end, the proposed mechanism divides each region into geographically distributed zones managed by cloud-fog nodes for charging service coordination. In each zone, we employ the Hungarian matching algorithm to optimally match EVs with the available charging services. Unlike recent approaches that establish a one-to-one matching between supplier EVs and demanding EVs, our mechanism matches multiple demanding EVs to charging services with a larger capacity to maximize the service offering. Comparing results with existing studies shows that our model outperforms prior approaches across critical factors. Furthermore, our proposed matching algorithm prioritizes EVs requiring charge based on their maximum travel range given their current State of Charge (SoC). To address the challenge of accurately estimating EV driving range, we introduce an ensemble-based Machine Learning (ML) model offering a compelling solution for enhancing the estimation of EV driving range for practical applications.

Acknowledgements

I extend my sincere gratitude to Dr. Abdulsalam Yassine, my supervisor, whose unwavering support has been integral to the completion of this thesis and research endeavor. His invaluable guidance, patient mentorship, and steadfast encouragement, particularly amidst the challenges posed by the pandemic, have been instrumental in shaping this work.

I am deeply thankful to Lakehead University and the Department of Electrical and Computer Engineering for their generous scholarships and awards, which have provided crucial financial assistance. Additionally, the provision of lab facilities and online remote desktop services has significantly enhanced my productivity and facilitated seamless progress in my research.

I am also indebted to my fellow lab mates whose camaraderie has made my research experience truly enjoyable. Our collaborative discussions on cutting-edge techniques and research trajectories have consistently enriched my understanding and perspective.

Table of Contents

List of Figures

List of Tables

List of Symbols

J – Set of DEVs.

K – Set of SEVs.

I – Set of FCSs.

H – Set of HCSs.

M – Set of MCSs.

L – Set of MLs.

p_k – Energy unit price determined by SEV k (¢/kWh).

p_0 – Original energy price (¢/kWh).

p_i – Energy unit price determined by FCS i (¢/kWh).

p_h – Energy unit price determined by HCS h (¢/kWh).

p_m – Energy unit price determined by MCS m (¢/kWh).

q_j – Requested quantity of energy of DEV j (kWh).

soc_j^r – Required state of charge of DEV j (%).

soc_j^c – Current state of charge of DEV j (%).

soc_k^a – Available state of charge of SEV k (%).

b_j^c – Battery capacity of DEV j (kWh).

c_k^b – Cost of battery degradation of SEV k (¢).

c_m^b – Cost of battery degradation of MCS m (¢).

$d_{j,l}$ – Distance between DEV j and ML l (km).

$d_{k,l}$ – Distance between SEV k and ML l (km).

$d_{j,i}$ – Distance between DEV j and FCS i (km)

$d_{j,h}$ – Distance between DEV j and HCS h (km).

$d_{j,m}$ – Distance between DEV j and MCS m location (km).

c_j^e – Energy consumption cost per kilometer of DEV j (kWh/km).

c_k^e – Energy consumption cost per kilometer of SEV k (kWh/km).

α – Value of time (¢/h).

v_j – Average speed of DEV j (km/h).

v_k – Average speed of SEV k (km/h).

λ – V2V energy transfer efficiency (%).

r^e – Rate of energy exchange per unit of time (kW).

c^r – Cost of replacing the battery (¢/kWh).

θ – Coefficient of battery capacity degradation (%).

Γ – Lowest acceptable threshold of the battery SOC (%).

$c^t_{j,l}$ – Cost of travelling DEV j to ML l (¢).

$c^t_{k,l}$ – Cost of travelling SEV k to ML l (¢).

c^{ti}_j – Cost of time of DEV j (¢).

c^{ti}_k – Cost of time of SEV k (¢).

t^w_j – Additional waiting time for DEV j (h).

c^s_j – Cost imposed on DEV j to compensate SEVs' cost (¢).

$c_{j,l}$ – Cost of charging DEV j with SEV k in ML l (¢).

$c_{j,h}$ – Cost of charging DEV j with HCS h (¢).

$c_{j,i}$ – Cost of charging DEV j with FCS i (¢).

$c_{j,m}$ – Cost of charging DEV j with MCS m (¢).

u^{ch}_j – Utility of seller in charging service (¢).

d^{th}_j – Maximum distance DEV j can go with current SOC (km).

δ – Threshold parameter (km).

t^{idle}_j – The idling time spent in traffic for DEV j (h).

t^{idle}_k – The idling time spent in traffic for SEV k (h).

List of Abbreviations

AI – Artificial Intelligence
CA – Correlation Analysis
CV – Cross-Validation
DEV – Demanding Charge EV
DSRC – Dedicated Short-Range Communication
EDA – Exploratory Data Analysis
ELM – Extreme Learning Model
EV – Electric Vehicle
FCS – Fixed Charging Station
GHG – Greenhouse Gas
HCS – Smart Home Charging Station
ICE – Internal Combustion Engine
ITS – Intelligent Transportation System
LR – Linear Regression
MAE – Mean Absolute Error
MCS – Mobile Charging Station
ML – Machine Learning
MLP – Multilayer Perceptron
MLR – Multiple Linear Regression
MP – Meeting Point
MSE – Mean Square Error
NN – Neural Network
PCA – Principal Component Analysis
R2 – R-Squared
RF – Random Forest
RMSE – Root Mean Square Error
RSU – Road Side Unit
RT – Regression Tree
SEV – Supplying Power EV
SOC – State of Charge
SVR – Support Vector Regression
V2G – Vehicle-to-Grid
V2H – Vehicle-to-Home
V2V – Vehicle-to-Vehicle
XGBoost – Extreme Gradient Boosting

I dedicate this work to my parents and spouse, not only for their financial assistance but also for their unwavering love and encouragement towards me.

Chapter 1

Introduction

The rapid growth of urbanization and the expansion of the social economy have led to a sharp increase in the number of vehicles in cities. Due to a lack of capacity, however, roadways become congested, which causes a number of problems, such as traffic accidents and environmental pollution [1]. In this evolving landscape, EVs are poised to emerge as the primary choice for transportation, gradually replacing conventional Internal Combustion Engine (ICE) vehicles [2]. EVs offer numerous advantages over their ICE counterparts, including the utilization of renewable energy sources, reduced dependence on fossil fuels, and zero Greenhouse Gas (GHG) emissions [3]. Indeed, given the urgent and growing concern of global warming, EVs, through harnessing renewable energy reservoirs, play a critical role in reducing GHG emissions, thereby combating the adverse impacts of climate change [3, 4]. The utilization of renewable energy not only helps mitigate the environmental footprint of transportation but also fosters energy security and independence by reducing dependence on volatile fossil fuel markets.

As a result, EVs have attracted a surge in attention from both industrial stakeholders and academic researchers. Their potential to revolutionize transportation by offering cleaner, more sustainable alternatives to traditional ICE vehicles has spurred innovation and investment in the EV sector. Furthermore, the expanding EV market has stimulated advancements in battery technology, charging infrastructure, and energy management systems, driving down costs and improving performance. As societies embrace a greener, more sustainable future, EVs stand poised to play a pivotal role in driving this transformative shift toward cleaner, more environmentally friendly transportation systems. Their widespread adoption represents not only a technological evolution but also a fundamental reimagining of how we move people and goods in a manner that is both ecologically responsible and economically viable.

Looking toward the future, the trajectory of EV adoption appears promising. Projections suggest that by 2030, there could be approximately 250 million EVs available annually, driven by national goals and increasing consumer demand [2]. The proliferation of EVs is expected to play a pivotal role in addressing climate change, as they employ renewable energy sources to reduce GHG emissions [3], [4].

In response to these evolving dynamics, governments worldwide are rolling out policies aimed at accelerating the transition to EVs. Nations such as Canada, the UK, and the United States have set forth ambitious targets to phase out ICE vehicles and incentivize the adoption of zero-emission alternatives [2, 5, 6]. Furthermore, proactive measures like China's decision to halt new investments in ICE production underscore a palpable shift towards the widespread adoption of EVs [2, 5, 6].

The International Energy Agency (IEA) envisions a rapid expansion in the deployment of EVs across global transportation networks, with expectations of a substantial reduction in carbon emissions by the year 2050 [3]. This impending transformation holds the promise of delivering significant benefits for power grid economics, fostering heightened resilience, reliability, and sustainability [6].

1.1 Technical Challenges and Motivations

Although EVs are becoming more popular, the widespread adoption of EVs faces significant obstacles. In the following, we will outline some of the technical challenges and discuss the motivations behind addressing them. These challenges include range limitations, extended charging times, and limited accessibility to FCSs [7–9]. Overcoming these challenges will be crucial in realizing the full potential of EVs as a greener and more sustainable mode of transportation.

Range anxiety, the concern that EV batteries may not provide sufficient range for desired travel distances, stands as a major deterrent to widespread EV adoption. Despite offering several incentives to entice people to purchase EVs, many users are still hesitant to buy EVs because of range anxiety, while the price of higher-range EVs is beyond the reach of average users [10]. This concern is particularly pronounced in rural and highway areas where charging infrastructure is sparse, leaving drivers uneasy about their EV's range capabilities.

Addressing range anxiety necessitates the development of a robust and accessible charging infrastructure, crucial for accelerating EV adoption [10]. Additionally, to facilitate the transition to EVs, electrical utility firms must invest in upgrading their network

infrastructure and generation capacity [11], [10]. By reinforcing the resilience and reliability of the power grid, such investments can support the seamless integration of EVs into the transportation ecosystem, thereby fostering sustainability and reducing carbon emissions.

To mitigate this range anxiety, it is essential to address two contributing factors that exacerbate this concern. Firstly, there is an issue with the inadequate and uneven availability of FCSs. Secondly, there is uncertainty surrounding the remaining range of EVs, which intensifies anxiety among EV owners to rely on EV batteries over the long term.

In the case of the former, a swift and effective solution involves the widespread deployment of FCSs throughout the entire nation. However, the deployment of FCSs is currently constrained to urban areas, where users often encounter long waiting times for EV charging [12]. In rural and remote regions, the range anxiety issue is exacerbated due to the high installation expenses associated with FCSs, extended travel distances, and inadequate electrical grid coverage. Nevertheless, the substantial upfront costs and the geographic remoteness of these areas may render the development of FCS networks challenging and potentially unprofitable [10].

Furthermore, relying solely on FCSs presents several challenges, including high installation costs and geographical constraints that may hinder network expansion, possibly making such efforts economically impractical. Moreover, the widespread deployment of FCSs has implications for electricity distribution systems, potentially inducing new peak loads and compromising power quality [13], [14], [15]. This could lead to power outages, increased recharging demands, and undesirable harmonic distortions, all of which pose risks to system reliability and efficiency [11], [10].

On the other hand, addressing the latter challenge, uncertainty in the remaining range of EVs, research aims to explore advanced methods for accurately predicting the driving range of EVs. Achieving a high level of predictive accuracy is paramount to instill confidence in EV drivers, allowing them to plan their journeys with certainty and rendering range anxiety a thing of the past. Concurrently, the precise prediction of EV driving range has emerged as a pivotal research domain, given its significant implications for vehicle usability and efficiency. This is precisely where ML models step into the forefront of research [16].

1.2 Research Approach

This study aims to tackle the technical challenges outlined earlier. This begins with developing a suite of auxiliary technologies to bolster FCSs networks. One promising solution involves exploring the bidirectional energy transfer capabilities of EVs, particularly through V2V technology. This innovative concept allows for the exchange of energy between EVs equipped with bidirectional energy transfer capabilities, such as the Ford 150 Lightning, effectively transforming them into mobile energy sources and reducing dependence on fixed charging infrastructure [13, 17]. In practical terms, when an EV faces a low charge and no nearby FCSs are available, a second EV with a surplus charge can step in to provide the required energy through V2V technology [7]. As a result, V2V technology emerges as a pivotal advancement towards realizing a highly secure and efficient Intelligent Transportation System (ITS) [18–20]. By empowering EVs to function as independent energy providers, detached from fixed charging infrastructure and grid connections, V2V technology fosters the development of a viable commercial ecosystem. This becomes particularly pertinent in scenarios where establishing permanent infrastructure proves economically unfeasible [10, 21].

The practical implementation of V2V charging offers mutual benefits to both EVs with charging needs, known as Demanding Charge EVs (DEVs), and those with excess charge, referred to as Supplying Power EVs (SEVs). These benefits include seamless energy transfer, reduced energy consumption when traveling to remote FCSs, and substantial energy trading opportunities [11]. Furthermore, V2V mode provides greater temporal flexibility, alleviating concerns about extended waiting times at FCSs [3, 4].

Similar to V2V, MCSs are also gaining attraction as a charging service for roadside assistance making it a viable cost-effective and feasible alternative where charging stations are not within reach [10], [21]. Indeed, V2V and MCSs bring flexibility and eliminate the problem of prolonged charging times at FCSs [3], [4]. Such features make V2V and MCSs an efficient highly secure technology for the future ITS [18], [19], [20].

This work innovative mechanisms whereby different EV charging options co-exist to help users eliminate range anxiety and maximize their benefits. In reality, while V2V technology holds promise, relying solely on it may not fully supplant fixed on-route charging service providers like FCSs to accommodate the growing EV adoption. As a response, our research introduces a model that integrates V2V with other charging services, including smart homes equipped with charging stations and charging service providers termed as HCS, along with MCSs.

One of the main challenges in this model is how to effectively match DEVs with the available charging services from HCSs, FCSs, SEVs, and MCSs. This study proposes a

novel matching mechanism where EVs utilize V2V, FCS, HCS, and MCS in a cooperative fashion to supply the required charging service. The proposed mechanism divides the available charging services into geographically distributed zones, and then employs a Hungarian matching algorithm to optimally match EVs with the available charging services. To facilitate the service seamlessly, we propose a cloud-based architecture where cloud-fog nodes assist in making the right decision for users to access the most suitable charging service in near-real time [22], [23].

This research also endeavors to confront the uncertainty surrounding the remaining range of EVs. To achieve this, an ensemble-based ML model will be developed, capable of accurately estimating the remaining range of EVs under various driving conditions and environmental factors. This precise estimation will be integrated into the proposed matching algorithm, which aims to prioritize EVs in need of charge based on their estimated remaining range. By incorporating this precise estimation into the algorithm, we can effectively identify and prioritize EVs with shorter remaining range, thereby alleviating their heightened range anxiety and ensuring efficient utilization of charging resources.

ML is a part of Artificial Intelligence (AI) that has changed many different industries by using data to make smart predictions. When it comes to EVs, ML plays a pivotal role in developing models adept at accurately predicting several parameters related to EVs such as energy consumption prediction, traffic congestion prediction, vehicle range prediction, etc. Regarding EV range prediction, these models analyze diverse factors such as battery health, driving history, environmental conditions like weather and traffic, drive cycle patterns (including speed profiles, braking, and acceleration frequency), battery temperature, and auxiliary power usage (e.g., air conditioning, lighting, horn usage). By synthesizing these multifaceted variables, ML models provide precise estimations of the remaining range of EVs without requiring recharging [24–26]. Indeed, EV range estimation is a complex problem influenced by numerous variables and this ML approach aims to capture these intricacies [27, 28].

In the realm of EV range prediction, the utilization of big data holds significant importance for building robust models. Hence, this study emphasizes the exploitation of feature engineering and the generation of meaningful features through extensive data analytics encompassing 35,000 data points, aimed at enhancing the prediction accuracy of the models. Many contemporary algorithms prioritize the generation and analysis of extensive datasets to enhance accuracy and performance [29]. With the increasing proliferation of EVs and the urgent necessity to alleviate range anxiety among EV users, precise and dependable driving range estimation assumes paramount importance. Big data facilitates the incorporation of a diverse range of factors, including real-time traffic

conditions, weather variations, and driver behavior, all of which influence energy consumption and, consequently, the driving range. Leveraging a large dataset empowers ML models to discern intricate patterns, adapt to dynamic driving scenarios, and furnish more accurate predictions.

1.3 Major Contributions

The main contributions of this thesis are:

- Proposing a fog-based architecture where charging services are managed in different geographical zones to facilitate coordination and information exchange during the charging matching process. This is significant because in suburban and rural areas charging services may sporadically exist. Therefore, fog nodes that are close to the charging service can coordinate the exchanging of energy between adjacent zones and control the excess or shortage of energy in each zone in order to maximize the number of charged EVs resulting in reducing range anxiety.
- Developing an approach for optimizing EV charging services through a novel matching algorithm and addressing various practical scenarios. The algorithm is based on cooperation between SEVs, FCSs, HCSs, and MCSs and considers available charging services to achieve optimal matching for charging DEVs. It selects the most suitable charging spot while considering constraints such as distance and availability, thereby minimizing DEV costs while maximizing charging rates. Furthermore, the proposed approach addresses practical scenarios based on the number of DEVs and available charging services in each zone.
- Developing a mechanism that reduces the waiting time for DEVs to be charged by considering the maximum capacity of each charging service. Waiting time is an essential factor that should be reduced during the matching process. Decreasing this time brings about decreasing cost for the DEVs as well as increases the satisfaction of users.
- Integrating the ML techniques to accurately predict EV range utilized for prioritizing DEVs during the matching algorithm, thereby reducing range anxiety and facilitating EV adoption. By considering factors like tire type, road condition, and driving style, the study enhances prediction reliability. Diverse ML models are employed and CV employment ensures robust evaluation. Utilizing a large dataset, real-world experiments demonstrate practical applicability, while scalability is enhanced by incorporating data from various EV models.

1.4 Publication

Published

- Hosseini, S. and Yassine, A., 2022, December. A novel V2V charging scheme to optimize cost and alleviate range anxiety. In 2022 IEEE Electrical Power and Energy Conference (EPEC) (pp. 354-359). IEEE.
- Hosseini, S., Yassine, A. and Akilan, T., 2024, March. Ensemble-Based Robust Model for Accurate Driving Range Estimation of EVs Leveraging Big Data. In 2024 IEEE 8th Energy Conference (ENERGYCON) (pp. 1-6). IEEE.

1.5 Organization

This thesis is organized as follows:

- Chapter 1: Introduction -This chapter provides an overview of the thesis, outlining its scope and key aspects.
- Chapter 2: Background and Related Work - This chapter offers brief descriptions of fundamental concepts essential for understanding the thesis. It covers topics such as V2V energy trading, bidirectional energy transfer capability in EVs, the Hungarian matching algorithm, non-sequential regression ML model, and K-fold CV. Additionally, it provides summaries of related work in the field, including V2V energy trading in smart grids and recent EV remaining range prediction studies.
- Chapter 3: System model and problem formulation - This chapter presents the overall architecture of the proposed system model. This chapter also describes the formula used in the proposed matching algorithm in our proposed system model.
- Chapter 4: Driving range estimation with ensembled ML model -This chapter focuses on the development of an ensemble ML model aimed at accurately predicting the range of EVs. Within the framework of our proposed matching algorithm, we prioritize EVs requiring charge based on their maximum attainable distance with their current SoC. Consequently, the ensemble ML model, developed for precise range prediction, serves as a pivotal tool in prioritizing EVs effectively.
- Chapter 5: Cooperative fog-based en-route EV charging service - This chapter proposes a novel matching algorithm based on Hungarian algorithm. It describes how multiple charging services collaborate to optimize critical factors while charging EVs. The chapter elaborates our proposed algorithm, complemented by thorough discussions on simulation outcomes and numerical results.
- Chapter 6: Conclusion and Future Work - This chapter summarizes the conclusions drawn from the thesis analysis and suggests potential future extensions to address current limitations.

Chapter 2

Background and Related Work

In this chapter, we delve into the fundamental concepts utilized in our proposed system, as outlined in Section 2.1. Following this, we provide a review of existing studies pertaining to V2V energy trading and the integration of AI for predicting the remaining range of EVs, as detailed in Section 2.2.

2.1 Background

In this section, we begin by discussing the concept of V2V energy trading, followed by an exploration of EVs equipped with bidirectional energy transfer capability. Then, we discuss the Hungarian matching algorithm used as a part of our matching algorithm. Afterward, we review the concepts related to non-sequential regression ML models and K-fold CV.

2.1.1 V2V energy trading

The V2V concept revolves around the interaction among EVs, enabling EV owners to potentially sell their surplus energy to other vehicles to help meet energy demands. V2V energy exchange can occur anywhere and at any time, offering greater flexibility. However, effective energy management solutions are still required to efficiently allocate potential excess energy and fulfill the energy needs of EV users. The motivation for participating in V2V frameworks varies; EVs in need of energy are primarily driven by the desire to meet their energy requirements, while those providing energy may be motivated by monetary rewards or reciprocal altruism [30], [31]. EVs with surplus energy and available time can exchange energy given that they are adequately compensated. Moreover, this can be extended to a business model where the energy provider serves

multiple EVs. Reciprocal altruism is another motivation, where an EV sells its energy to another EV in need, with the expectation of receiving similar assistance in the future [12].

Carefully designed mechanisms for intelligent charging and discharging behavior are essential for realizing efficient and effective V2V solutions. Various aspects of the V2V charging problem must be considered, including users' privacy, data security, and cost and profit models, before developing complete V2V solutions. Current research endeavors in V2V solutions tackle a range of challenges, spanning several focal points such as charging price optimization [32], [33], [34], efficient consumer/provider matching [8], [15], [35], and user privacy and data security management [36], [37], [38]. The first research problem focuses on optimizing charging costs for EVs by finding the optimal schedule to reduce charging costs based on forecasted electricity prices while meeting EVs' charging requirements [32], [34]. The second research problem aims to achieve efficient and feasible matching between consumers (EV users requesting energy) and providers (EV users with surplus energy willing to trade for profit), reflecting on factors such as total charging cost, projected profit, system social welfare, or individual rationality of EV users [8], [35]. The final research problem concentrates on developing solutions to protect user privacy and data. Our research focuses on optimizing consumer/provider matching, where our algorithm carefully weighs charging costs, supplier profits, time, and charging rates while integrating cutting-edge technologies like AI into the matching process.

2.1.2 EVs equipped with bidirectional energy transfer capability

EV battery chargers are categorized into on-board and off-board charging systems, with options for unidirectional or bidirectional power flows [39]. Unidirectional systems are preferred for their minimal hardware requirements, simplified interconnection, and lower risks of battery degradation. Conversely, bidirectional systems offer distinct advantages like power stabilization, Vehicle-to-Grid (V2G) technology integration, and controlled power conversion. For instance, Level 3 high-power charging systems, especially those equipped with three-phase bidirectional multilevel converters, are highly favored due to their numerous benefits, including superior power quality, reduced harmonic distortion, improved power factor, reduced electromagnetic interference noise, and consistent DC output voltage [40].

The integration of bidirectional chargers in EVs unlocks various features and benefits, with a notable emphasis on V2G technology. In V2G scenarios, EV batteries can feed energy back to the grid during periods of low usage, thereby bolstering grid efficiency

and stability. This capability enhances overall grid reliability and fosters a more resilient power infrastructure. Moreover, bidirectional power flow facilitates other applications such as V2V and Vehicle-to-Home (V2H). In the V2V scenario, local communities of EVs can be established, allowing for the exchange of energy among vehicles for charging and discharging purposes. These applications highlight the versatility and potential of EVs with bidirectional power capabilities in contributing to energy management and grid stability [40], [41], [42].

Bidirectional charging necessitates both compatible chargers and vehicles capable of two-way charging. Even with a bidirectional charger equipped with its converter, the functionality relies on the presence of vehicles capable of utilizing this feature effectively. Notable examples of EVs equipped with bidirectional transfer capability include the Nissan Leaf ZE1, Outlander PHEV, Hyundai Ioniq 5, KIA EV6, BYD Atto 3, BYD Han EV, Ford F-150 Lightning, MG ZS EV (2022), and various VW ID Models. EVs equipped with bidirectional charging capabilities signify a substantial leap forward in the convergence of electric transportation and the wider energy ecosystem. Beyond merely consuming electricity, these vehicles play a dual role by also bolstering grid resilience, presenting diverse applications ranging from serving as backup power sources to actively engaging in demand response initiatives.

The V2V capability can be realized with a bidirectional wireless charging system, wherein the charger can transfer power from an energy source to a load, as well as from the battery load to the charging coil of another EV [41].Various methodologies for V2V wireless power transfer are explored in [43], [44]. In wired connections for V2V power transfer, both AC and DC charging equipment are utilized to charge an EV battery through V2V operations. The conventional method involves AC V2V charging, necessitating EVs equipped with on-board chargers and involving multiple conversion stages [32], [45]. However, DC V2V charging is also feasible, employing either on-board [46], [47] or off-board [48], [49] charging systems for EVs [50].

2.1.3 Hungarian Matching algorithm

In his renowned paper titled, The Hungarian method for the assignment problem [51], Harold W. Kuhn introduced an algorithm for constructing a maximum weight perfect matching in a bipartite graph. Kuhn charmingly recounts in his memoirs how the insights of two Hungarian mathematicians, D. K Ìonig and E. Egerv Ìary, dating back to 1931, inspired the development of his algorithm, which he aptly named the Hungarian method [52].

The assignment problem, also known as the maximum weighted bipartite matching problem, is an extensively studied problem with applications in various domains [53]. It can be defined as follows: given a group of workers, a set of jobs, and a series of ratings indicating each worker's suitability for each job, the objective is to determine the optimal assignment of workers to jobs, maximizing the total rating [54].

The Hungarian algorithm solves the assignment problem in $O(n^3)$ time, where n is the size of one partition of the bipartite graph. Existing algorithms for solving the assignment problem assume the existence of a matrix of edge weights w_{ij} or costs c_{ij}, and the problem is addressed based on these values. In cases where the sizes of the two partitions of the graph are unequal, a common strategy involves inserting dummy nodes with zero-weight edges to all nodes in the opposing partition [55]. Consequently, the Hungarian algorithm consistently yields a complete matching, although this matching may include zero-weight edges, representing no assignment. Each step of the Hungarian algorithm requires $O(n^2)$ arithmetic operations, and with the appropriate data structures, the computational complexity of the entire algorithm across n stages is $O(n^3)$. The Hungarian algorithm is provably complete and optimal [56]. We integrate the Hungarian algorithm into our proposed matching algorithm, and its details are outlined in Algorithm 1. This algorithm aims to match the entities of task 1 with those of task 2. For instance, it facilitates matching between a set of jobs (task 1) and a set of employees (task 2) [56].

2.1.4 Non-sequential Regression ML models

Recently, the utilization of ML has surged across various scientific domains, offering automated exploration of concealed patterns or correlations within datasets. This trend has notably extended to fields like nondestructive testing, objective detection, time series prediction, pattern recognition, and both classification and regression, thereby presenting an appealing alternative to minimize manual labor across diverse domains [57]. Among these, classification and regression stand out as specific forms of prediction and represent core research directions in ML, statistics, and data mining. In regression tasks, the primary objective is to train a model using available data to map inputs to corresponding output values, thereby facilitating predictions [58].

ML typically falls into two primary categories: predictive or supervised learning, and descriptive or unsupervised learning methodologies [59]. The following subsections offer a concise explanation of both categories.

Algorithm 1 Hungarian Matching Algorithm

Inputs :

1. Define the set of task 1 as $M = \{1, 2, ..., m\}$ and the set of task 2 as N=$\{1, 2, ..., n\}$.
2. Generate an $n \times m$ matrix known as the cost matrix. Each element in this matrix denotes the cost associated with assigning a member from the task 1 set to a member from the task 2 set.
3. **if** $n \neq m$ **then**
   3.1 Add columns or rows of zeros to the cost matrix so that there are at least as many columns as rows.
   3.2 Update m and n values.

end if

Steps :

1. **for** *each,* $i \in M$ **do**
   Subtract the lowest row value from each row.

end for

2. **for** *each,* $j \in N$ **do**
   Subtract the lowest column value from each column.

end for

3. Cover the zeros with as few lines as possible.

3.1 **if** *Number of Lines*= $Max(m, n)$ **then**
   Go to Step 4.

else
   3.2 Find the minimum number of the cells that are uncovered.
   3.3 subtract that value from all uncovered cells.
   3.4 Add that number to the cells wherever two lines intersect.

end if

4. Assignment of Zeros Sub-Algorithm

4.1 **for** *each,* $i \in M$ **do**
   if *a row has exactly one zero* **then**
      Assign it
   else
      leave the row for now
   end if
   4.2 If a cell has been assigned, close the row and column.
   4.3 **for** *each,* $j \in N$ **do**
      if *a column has exactly one zero* **then**
         Assign it
      else
         leave the column for now
      end if
      4.4 If a cell has been assigned, close the row and column.
   end for

end for

Output:

Final optimal assignment between members of task 1 and task 2 sets.

[1]

2.1.4.1 Supervised Machine Learning

Supervised ML, a widely employed technique, relies on guidance from a teacher or supervisor who provides precise error measurements. These measurements aid in adjusting parameters iteratively to minimize a global loss function. The process involves learning a mapping function from input variables to an output variable, using labeled examples from a dataset. The goal is to achieve accurate approximations of the mapping function for generalization to unseen samples. Supervised learning encompasses regression, focusing on predicting continuous values, and classification, which involves categorizing output variables [59].

2.1.4.2 Unsupervised Machine Learning

Unsupervised learning is distinguished by the absence of a supervisor, contrasting with supervised learning, which relies on a supervisor and an objective function for learning guidance. Algorithms in unsupervised learning autonomously explore data structures without predefined correct answers. The dataset comprises unlabeled examples, where each example is represented by a feature vector. The aim of unsupervised learning is to develop models that transform feature vectors into useful values or vectors for practical problem-solving, aiming to uncover interesting patterns within the data, a process known as knowledge discovery. Unlike supervised learning, there are no prescribed patterns to identify, and no explicit error metric to assess performance, making it a less well-defined problem. Unsupervised learning problems encompass clustering, which identifies natural groupings within data, and association learning, which uncovers insights, relationships, and frequent patterns among different objects in the dataset, such as rules indicating associations between items in transactional data [59].

2.1.5 K-fold Cross-Validation

K-fold Cross-Validation (CV) is one of the most common techniques for model evaluation and selection in ML practice. It uses a combination of multiple tests to obtain a stable estimate of the model error. This technique is particularly useful when there is not enough data for a hold-out CV. The available learning set is partitioned into k disjoint subsets of approximately equal size, where each subset is referred to as a fold. This partitioning is done by randomly sampling cases from the learning set without replacement. The model is trained using $k-1$ subsets, collectively forming the training set, and then applied to the remaining subset, denoted as the validation set, to measure its performance. This process is repeated until each of the k subsets has been used as a

validation set, ensuring that no two test sets overlap. The average of the k performance measurements on the validation sets yields the cross-validated performance. Algorithm 2 provides a detailed description of this method [59], [60].

Algorithm 2 K-fold CV

Inputs :
dataset T, number of folds k, performance function error, computational models $L_1, \ldots, L_m$, $m \geq 1$.
Steps :
1. Divide T into k disjoint subsets $T_1, \ldots, T_k$ of the same size.
2. **for** $i = 1, \ldots, k$ **do**
   2.1 $T_v \leftarrow T_i$, $T_{\text{tr}} \leftarrow \{T - T_i\}$.
   2.2 **for** $j = 1, \ldots, m$ **do**
      Train model L_j on T_{tr} and periodically use T_v to assess the model performance: $E_j^v(i) = \text{error}(L_j(T_v))$.
      Stop training when a stop-criterion based on $E_j^v(i)$ is satisfied.
   end for
end for
3. **for** $j = 1, \ldots, m$ **do**
   evaluate the performance of the models by: $E_j^v = \frac{1}{k} \sum_{i=1}^{k} E_j^v(i)$.
end for

[2]

As error measure functions, some of the common metrics used include Mean Squared Error (MSE), which quantifies the average squared difference between predicted and actual values; Root Mean Squared Error (RMSE), the square root of MSE, providing a measure of error magnitude; Mean Absolute Error (MAE), calculating the average absolute difference between predicted and actual values; and R-Squared (R2) Score, indicating the proportion of variance in the dependent variable predictable from the independent variable. The following equations represent the formulas for these error metrics.

Mean Squared Error (MSE):

$$\text{MSE} = \frac{1}{n} \sum_{i=1}^{n} (y_i - \hat{y}_i)^2 \tag{2.1}$$

Root Mean Squared Error (RMSE):

$$\text{RMSE} = \sqrt{\text{MSE}} \tag{2.2}$$

Mean Absolute Error (MAE):

$$\text{MAE} = \frac{1}{n} \sum_{i=1}^{n} |y_i - \hat{y}_i| \tag{2.3}$$

R-squared (R2) Score:

$$R^2 = 1 - \frac{\sum_{i=1}^{n}(y_i - \hat{y}_i)^2}{\sum_{i=1}^{n}(y_i - \bar{y})^2} \tag{2.4}$$

where n is the number of observations or data points, y_i represents the actual observed value for the ith data point, $\hat{y}_i$ represents the predicted value for the ith data point, and $\bar{y}$ represents the mean of the observed values y_i for all data points.

2.2 Literature Review

The literature contains numerous studies focusing on V2V energy trading systems, with particular attention given to the development of energy management protocols aimed at optimizing and regulating charging decisions for pairs of SEVs and DEVs. Furthermore, as highlighted earlier, accurately predicting an EV's remaining driving range is crucial for alleviating range anxiety among drivers. To tackle this challenge, several research efforts have concentrated on devising methods to estimate EV driving range using ML models. For clarity, we categorize this section into two subsections: V2V energy trading in smart grids and EV Remaining Range Prediction, where we provide detailed insights into relevant works for each subsection.

2.2.1 V2V Energy Trading in Smart Grids

This subsection sheds light on the most significant related studies, highlights the main shortcomings, and provides a comparison with the proposed work on V2V energy trading in this thesis.

Authors in [33] present a communication framework based on VANETs, along with two mathematical models and an optimization-based V2V charging strategy. They use a distributed parking place reservation and centralized charging-discharging matching scheme, as a first-come first-served technique, to reduce charging costs, improve energy exchange efficiency, and coordinate the movement of EVs. However, the study falls short in addressing the problem of maximizing the rate of charged EVs. The study in [3] suggests a two-layer matching approach for a practical V2V optimization model. It employs the Gale-Shapley game to produce stable matching between EVs and devises a user satisfaction model to efficiently select EV pairs that obtain high user satisfaction. The study considers aspects such as invested time, user satisfaction, system energy efficiency, and social welfare, as well as the cost and profit of EV users. In [15] and [35], researchers provide a flexible V2V matching algorithm-based energy management plan

that incorporates various V2V matching algorithms, such as a weighted bipartite graph, max-weight, and stable algorithms, to achieve some objectives, such as maximizing social welfare and minimizing costs, by employing a weighted bipartite graph. This work, however, does not consider nearby charging stations and only considers a specific case of V2V energy trading where the number of DEVs and SEVs is equal. The work in [36] suggests utilizing bichromatic mutual nearest neighbor assignments to efficiently match consumer EVs with supplier EVs using V2V technology while maintaining privacy. The matching algorithm assigns participants in a way that satisfies all parties involved in the dynamic environment by allowing users to join or leave. The algorithm aims to decrease the average user waiting time until they are matched.

An innovative energy trading strategy between two pairs of EVs is suggested in [34] predicting the daily schedule and travels of a synthetic population for Flanders (Belgium) using an activity-based approach, which greatly decreases the effect of the charging process on the power system and benefits financially all users participating in the trading process. Other studies such as [21], [61], and [32] have concentrated on developing charging as well as energy management protocols based on using V2V along with vehicle-to-other charging services to regulate and optimize the charging of EVs. The authors in [32] suggest an offline optimal Mixed Integer Programming which validates the efficacy of employing optimal EV charging schedule strategy with the choice of V2G and V2V energy transfer. The strategy of energy transfer aims at enhancing energy utilization and improving customer satisfaction. The work in [62] proposes an adaptive learning approach for grid-connected charging station optimization, showing robust performance in simulations under diverse conditions, including stochastic arrival/departure times and various pricing models, with consideration for solar energy production. However, they do not focus on charging costs and the rate of charging EVs.

Parallel to the studies mentioned above, several research efforts emphasize on mitigating range anxiety by increasing the number of charged EVs. For example, the work in [10] develops a V2V energy transfer mechanism to increase the number of charged EVs using a limited number of charging trucks outfitted with a larger battery and a fast charger. The work in [7] introduces a V2V charging architecture that matches supplier EVs with EV drivers experiencing range anxiety using a maximum-weighted matching algorithm managed by a location-based social networking system. It offers EV drivers complete control while protecting their privacy. The study in [61] addresses methods for optimizing charging strategies by proposing an algorithm based on matching theory. The goal is to enable efficient collaboration between vehicle-to-charging station and V2V charging systems while providing adequate charging services for EVs.

Studies such as [63], [64], [65], [7], and [36] focus on investigating the privacy concerns arising from the process of V2V charging. Researchers in [63] introduce a new consensus mechanism and employ a Stackelberg game model-driven incentive mechanism to maximize the benefits of both sellers and buyers to reduce the cost of buyers and increase the utility of sellers. The V2V system in work [64] ensures the protection of privacy for EVs when they are charging and discharging energy, maintaining the confidentiality of their location, time, and energy consumption details.

Study [66] suggests the establishment of an energy trading market for EVs that operates on a double auction mechanism to improve social welfare. The main objective is to facilitate the matching of consumers and providers within this market, with the ultimate goal of maximizing the system payoff while ensuring the privacy of all participants. In study [67], the authors propose an electricity trading architecture, utilizing blockchain technology, that enables V2V and V2G transactions. This architecture ensures secure information recording on the blockchain ledger. By incorporating a Bayesian game framework, they introduce a two-way auction mechanism and a novel price adjustment strategy, aiming to enhance social welfare and cost performance for both parties engaged in energy trading.

Despite their advantages, one of the limitations of the above V2V energy-sharing methods is that during the matching process, they do not take into account both the benefits of sharing energy and the need to alleviate range anxiety simultaneously. In [21], researchers propose a trip-based probabilistic EV charging behavior model and a V2V energy-sharing coordination technique. The proposed technique has three objectives: maximizing the number of EVs matched with energy suppliers, prioritizing EVs with surplus energy over charging stations during peak hours to alleviate energy demand from the grid, and prioritizing supplier EVs with lower detour costs when multiple matches involve the same number of supplier EVs. However, the authors consider a one-to-one approach when assigning EVs. This means that each SEV can supply just one DEV. In addition, it does not consider the charging cost as a performance measurement in the simulations. Work [68] introduces a joint optimization problem to maximize social welfare, addressing both the determination of unit prices and winners through a truthful double auction approach. Additionally, the aim is to maximize the rate of EV charging by purchasing energy from the power grid for auction losers. The study [69] introduces V2V wireless power transfer, addressing hurdles in EV adoption like high battery costs, insufficient charging infrastructure, and limited range. It evaluates V2V WPT performance in three real scenarios, considering its potential to reduce EV battery sizes and costs while enhancing system-wide energy savings to serve as much demand as possible.

TABLE 2.1: Comparison between our work and existing studies for V2V energy trading

Objectives	[33]	[3], [15], [35]	[36], [65]	[21] [69]	[32]	[10]	[7]	[61]	[63]	[66]	[67]	[68]	This Work
Minimizing Charging Cost	✓	✓	–	✓	–	–	–	–	✓	✓	✓	✓	✓
Maximizing the Rate of Charged EVs	–	–	–	✓	–	✓	✓	✓	–	–	✓	✓	✓
Minimizing the Waiting Time	✓	–	✓	–	–	–	–	–	–	–	–	–	✓
Cooperation between EVs and other charging services	–	–	–	✓	✓	–	–	✓	–	–	–	✓	✓
One-to-multiple approach when applying V2V	–	–	–	–	–	–	–	–	–	–	–	–	✓
Using Maximum Capacity of charging services	–	–	–	–	–	–	–	–	–	–	–	–	✓
Privacy-preserving Energy Trading Scheme	–	–	✓	–	–	–	✓	–	✓	✓	✓	–	–
Employing Auction-based V2V Matching	–	–	–	–	–	–	–	–	–	✓	✓	✓	–

The authors in [70] introduce a V2V WPT framework that enables EVs with low battery charge to link with high-charge vehicles while traveling in a platoon, eliminating the need for stops at charging stations and dynamically extending EVs' driving range.

None of the above-mentioned studies employ a one-to-multiple approach when assigning SEVs and DEVs together. In our earlier study [71], we evaluated the V2V trading system by taking into account a model with several zones where DEVs and SEVs would match together in a one-to-one method to swap energy in a way of minimizing the cost of DEVs as well as decreasing the range anxiety. Expanding on our previous work, this thesis proposes a novel cooperative mechanism where EVs can access charging services such as V2V charging schemes, private HCS, or MCS to complement existing FCS services in certain regions. To better compare our work with existing studies, we summarize in Table 1 the main aspects/categories that differentiate our work from previous studies that are closely related to ours. Notably, "this work" refers to the development of a matching algorithm concerning energy trading within smart cities.

2.2.2 EV remaining range prediction

Accurately predicting an EV's remaining driving range is crucial for alleviating range anxiety, especially among EV owners with limited remaining range. Prioritizing Dynamic EVs (DEVs) based on their remaining charge can help address this issue, necessitating the development of an accurate EV range prediction method. To tackle this challenge, several research efforts have concentrated on devising methods to estimate EV driving range using ML models. Additionally, modeling an EV's energy consumption is essential for predicting its driving range, leading to two approaches for addressing range anxiety: predicting energy consumption rates and directly predicting the remaining driving range of EVs.

2.2.2.1 Predicting the EV energy consumption rate

Numerous studies in the literature have focused on external factors affecting energy consumption in EVs. These factors include temperature, auxiliary loads (such as lighting and air conditioning), and road gradient, as explored in [72], [73], and [74]. However, relying solely on external factors may not always yield precise results due to the challenge of comprehensively considering all external variables. Moreover, driver behaviors, including driving patterns, speed, and acceleration, also play a significant role in energy consumption.

Authors in [28] and [75] address EV range anxiety. The former combines real-world driving data with geographic and weather information to predict energy consumption, using Multiple Linear Regression (MLR) and a Neural Network (NN) to forecast driving parameters. The latter suggests using Linear Regression (LR), Support Vector Regression (SVR), and an NN to connect future energy consumption to factors like velocity, elevation changes, and past consumption. Both works focus on improving EV range predictions through data-driven approaches, with the former emphasizing real-time driving parameters and the latter exploring future energy consumption factors.

In [76], a data-driven approach focuses on predicting EV demand through the analysis of vehicular traffic data between origin-destination pairs, estimating energy consumption per trip. [25] introduces a hybrid ML model for predicting EV trip power consumption, incorporating historical trip features and a modified self-organizing map with Regression Trees (RT). [77] presents a probabilistic Bayesian approach to predict energy consumption for road links and routes, enabling planning within a confidence interval, and addressing energy demand uncertainty. These works collectively explore data-driven approaches to enhance EV energy prediction, emphasizing different aspects like demand, power consumption, and probabilistic modeling. While [76] focuses on demand prediction, insights from [25] and [77] could complement the broader understanding of energy consumption modeling and its challenges.

2.2.2.2 Predicting direct EV driving range

Over the past decade, ML-based approaches have been employed for the direct remaining driving range prediction of EVs. These approaches aim to enhance range prediction, reduce driver anxiety, and improve energy management. For instance, the works [24], [16], [78], and [79] primarily propose data-driven approaches for EV range prediction. Authors in [24] introduce an innovative approach by proposing a blended ML model designed to predict the remaining driving range of EVs based on historical driving data.

TABLE 2.2: Comparison between our work and existing studies for EV range prediction

Objectives	[24], 2020 [78], 2014 [28], 2017 [25], 2023	[82], 2021, [27], 2019, [83], 2015	[16], 2021,	[81], 2023	[80], 2019	[72], 2018 [73], 2017 [74], 2017	[75], 2014	This Work
Addressing diverse factors affecting EV range	✓	✓	✓	✓	✓	–	–	✓
Choosing various ML algorithms	–	–	–	✓	✓	–	✓	✓
Using a factor to compare ML models	–	–	–	–	✓	–	–	✓
Applying big data analysis	–	✓	–	–	–	–	–	✓
Applying criteria: accuracy, overfitting, inference time	–	–	–	–	–	–	–	–
Using data from real vehicles	✓	✓	✓	✓	✓	✓	✓	✓

They use two advanced ML algorithms, namely XGBoost and light XGBoost to find the relationship between driving distance and a set of chosen features. These features include the cumulative output energy of the motor and the battery, different driving patterns, and the temperature of the battery. The study presented in [16] deploys the MLR for predicting the EV range. It underlines the significance of data-driven solutions and highlights the potential of ML in improving the accuracy of EV range estimation. Similarly, the model in [78] focuses on computing the confidence level that a driver can reach a particular destination with the available battery charge of the EV. It accounts for various sources of estimation uncertainty, including the driver, environment, auxiliary systems, and vehicle battery. The model uses efficient feature-based LR, providing real-time updates for an attainability map. The authors in [79] propose a data-driven approach for range prediction that adapts to changing conditions in real-time, without relying on specific vehicle parameters. It uses ML techniques, specifically kernel adaptive filtering, to adapt to changing conditions in real-time. This approach is evaluated on data from nine vehicle trials, comparing it with other methods, including linear adaptive filters and neural networks.

The above literature does not thoroughly address the challenges and trade-offs in selecting specific ML algorithms, which is a critical aspect of model development. In contrast, [80] and [81] introduce a system to alleviate range anxiety in EV drivers through several ML models. For example, researchers in [81] attempt to alleviate range anxiety through ML and conduct a comparative analysis with various algorithms. They highlight the significance of model selection, which is an aspect not thoroughly analyzed in the earlier works. Hence, [80] applies MLR, MLP, deep MLP, RF, and AdaBoost ML models based on features, like average speed, route type, and driving style for driving range prediction accuracy.

A prevailing limitation in the mentioned research studies is the restricted dataset size. The works [83], [82], and [27] utilize big data approaches to mitigate this issue. In [83], a two-state solution is introduced. Firstly, it estimates battery pack life over 1600 cycles, considering vital battery factors. Secondly, it delves into EV driving pattern analysis, employing growing hierarchical self-organizing maps as a machine-learning technique to cluster extensive EV data. It uses hierarchical self-organizing maps to analyze EV

driving patterns, covering energy consumption, driving range, powertrain simulation, and driving behavior. In [82], the focus is on accurately predicting the remaining EV mileage using the XGBoost algorithm. It directly forecasts remaining mileage after preprocessing real driving data, achieving high accuracy. This model is further enhanced by expanding the dataset and adopting a model fusion strategy. In [27], the authors leverage gradient-boosting decision trees to improve driving range prediction. These works collectively tackle the challenge of enhancing range prediction for EVs. While [83] handles battery life estimation and driving pattern analysis, [82] and [27] focus on directly predicting remaining mileage. However, these works lack in-depth discussions of various ML models.

To better compare our work with existing studies, we summarize in Table 2.2 the main aspects/categories that differentiate our work from previous studies. It's important to note that in this table, "this work" refers to the development of an ML method aimed at predicting the range of EVs. This method is seamlessly integrated into our proposed matching algorithm designed for energy trading within smart cities.

In comparison to existing works, our study endeavors to predict the driving range of EVs by employing multiple ML models and harnessing a substantial dataset comprising 35,000 data points. This approach aims to bolster the robustness of our analysis while leveraging various ML methods to yield more dependable predictions. Furthermore, while previous research has primarily focused on specific models of EVs, our study broadens the scope by incorporating data from various EV models, thereby enhancing the breadth of analysis.

For instance, the methodology outlined in [80] lacks a comprehensive discussion on critical issues such as overfitting and inference time, merely presenting CV results. Additionally, the dataset utilized in their study is limited to approximately 3,000 instances. In contrast, our research addresses these concerns by thoroughly examining overfitting issues and reporting inference times to facilitate a comprehensive comparison between models. We evaluate the models based on three key criteria: accuracy, inference time, and overfitting, providing a more nuanced understanding. Moreover, we conduct a comprehensive evaluation using CV, as well as standard training and hold-out sets to ensure the development of a more reliable model.

Chapter 3

System Model and Problem Formulation

This chapter introduces the proposed fog-based system model, detailed in Section 3.1. This model is designed to manage charging services across different geographical zones, aiming to enhance coordination and information exchange during the charging matching process. In addition, in Section 3.2, we present the formulas related to the cost of DEVs and the utility of sellers in charging services, which are essential components of our proposed algorithm deployed within our system model for matching DEVs and available charging services.

3.1 System Model

The system model shown in Figure 3.1 consists of EVs, HCSs, FCSs, MCSs as IoT devices, and a fog computing-based control architecture. The system employs fog computing for communication, in which the three main components of the architecture are the cloud layer, fog layer, and IoT devices layer [84]. Several zones intersect in our system, and each zone is controlled by fog nodes to capture IoT data streams produced in real-time by IoT devices. The cloud layer conducts offline analysis and stores transaction history. The fog layer comprises fog nodes and fog controllers for decision-making and responding to charging requests from DEVs. Fog nodes, represented by Road Side Units (RSUs) installed at specific traffic lights within each zone, strategically cover designated areas, enabling local data collection and communication. Each RSU as a fog node will have a defined geographic area, and vehicles and charging services that are inside that area will automatically be associated with the fog node. These RSUs establish

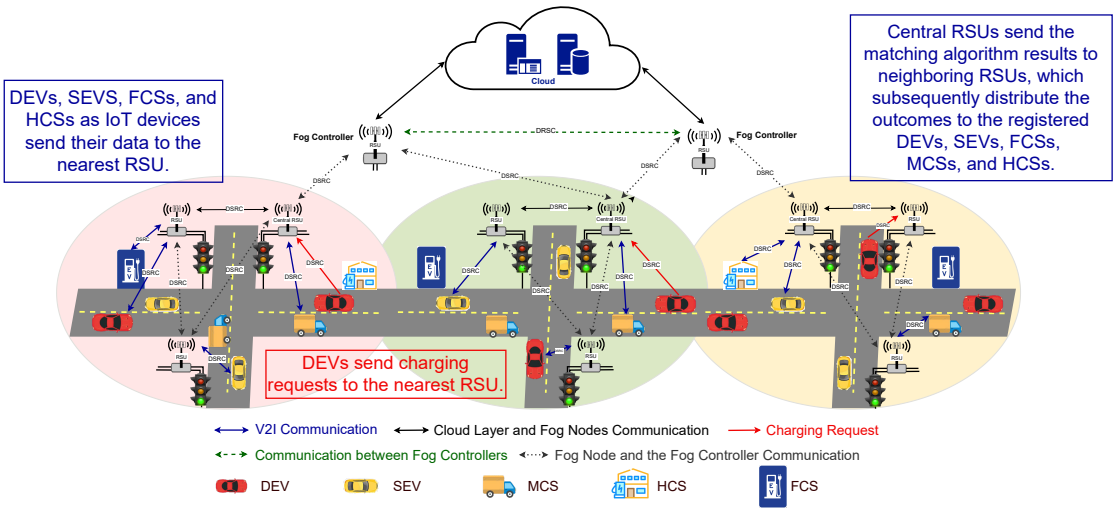

FIGURE 3.1: SEVs, DEVs, MCSs, FCSs, and HCSs in several zones are modeled as part of a system model for energy trading system managed by fog computing.

a mesh network, where each unit serves as a node capable of communicating with neighboring RSUs within its range. Equipped with Dedicated Short-Range Communication (DSRC) capabilities and ABB's software applications, RSUs efficiently gather data and commands from IoT devices via DSRC communication. ABB's software, operational on RSUs, conducts advanced analytics, including traffic congestion and energy consumption predictions. Among these RSUs, one functions as a central RSU, overseeing the final matching process. Following matching, the central RSU disseminates results to neighboring RSUs, which, in turn, relay this information to IoT devices within their vicinity, registered on those RSUs' database systems. Additionally, fog controllers, acting as specialized RSUs with gateway functionality, establish communication links between central RSUs in adjacent zones. Located at zone boundaries, these interconnection gateways ensure seamless connectivity and data exchange between RSUs, acting as communication bridges. The dedicated RSU with gateway functionality serves as a fog controller, managing inter-zone communication data routing, security features, and coordination with adjacent zones. In contrast, zone RSUs concentrate on intra-zone communication data processing tasks within their designated zones. The IoT devices layer encompasses EVs equipped with ABB's mobile application, and MCSs, HCSs, and FCSs equipped with ABB's charging station management software. This layer is designed to gather data from diverse sensors such as GPS, speed sensors, and battery status sensors. All IoT devices within this layer utilize DSRC modules for wireless communication with nearby RSUs. Prior to connecting to the charging network, IoT devices are required to register in the system's database. EVs and MCSs initiate this registration process upon entering the proximity of an RSU.

Leveraging ABB software in our system model offers several advantages, including industrial compatibility and seamless integration across IoT devices and RSUs. The predictive capabilities embedded within ABB software, derived from analysis of historical data and sensor inputs, enhance calculation accuracy and improve the matching process, benefiting energy management and traffic flow. Addressing the challenges of scalability and resource management, our distributed architecture, characterized by decentralized decision-making, ensures effortless expansion and resource allocation as the number of IoT devices increases, while minimizing latency for real-time data processing. Moreover, the deployment of RSUs, exemplified by the AI-500-095 dual mode system, seamlessly integrating with the AI-500-085 controller in traffic lights, provides a practical solution with DSRC communication protocols for seamless integration into the fog-based architecture. Notably, as an illustration of the predictive capabilities embedded within ABB software utilized in RSUs for predicting some concepts such as energy consumption, traffic conditions, and the remaining range of EVs, we have developed an ML-based prediction model specifically for estimating the remaining range of EVs. This predictive model will play a key role in our proposed algorithm, where EVs will be authorized based on their estimated remaining range.

The gathered data from DEVs include the quantity of energy demanded, routes, locations, and speed, and the data from SEVs include location, availability, speed, and the amount and costs of energy supplied. The fog nodes also collect data from FCSs and HCSs regarding the location, availability, quantity, and cost of energy.

Moving EVs can be classified into two groups based on their SOCs and energy demands: SEVs and DEVs. The former can be encouraged by the sale of excess energy to DEVs for additional fees, while the latter should be matched to an appropriate supplier to demand energy for charging. The moving supplier EVs become accessible either at random known as SEV or as dedicated roadside assistance known as MCS. In our model, we classify SEVs as random charging services, and MCSs, along with FCSs and HCSs, as dedicated charging services. In the EV network, MCSs play a significant role as they can supply a substantial amount of external energy, surpassing the capacity of traditional SEVs. When its SoC approaches a threshold limit, the DEV submits the charging request to the nearest RSU through the ABB application. Utilizing our proposed matching algorithm, the RSU makes a decision to match this DEV with the appropriate charging service and transfers the results to EVs and charging services. DEVs paired with SEVs during the matching process require an available location for mutual charging, which can also serve as their designated Meeting Point (MP). For simplicity, in our model, we assume each MCS in each zone has a fixed meeting location where DEVs can go for charging. In this thesis, we use the term "MP" to denote the meeting point for SEVs and we use the term "MCSs location" to denote the meeting points for MCSs.

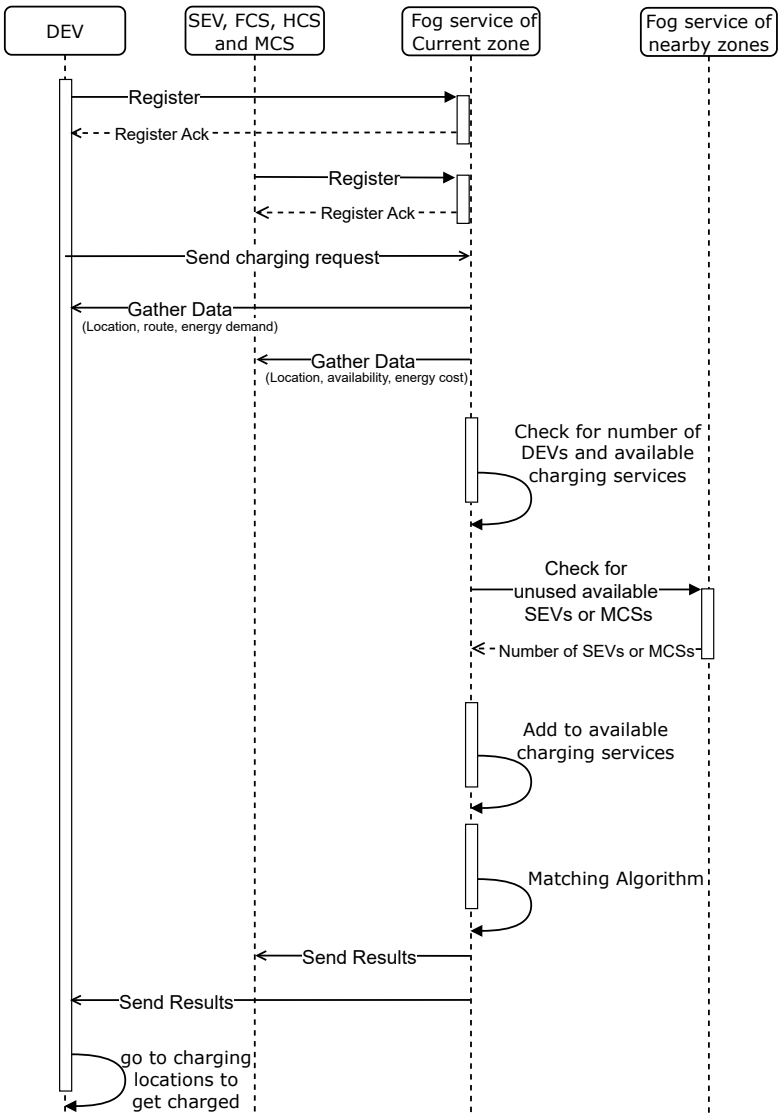

FIGURE 3.2: Sequence Diagram for SEVs, DEVs, MCSs, FCSs, HCSs, and zones services.

During the decision-making stage, the central RSU assigned to a particular zone utilizes a matching algorithm called the Hungarian algorithm to pair DEVs with SEVs when receiving charging requests from DEVs with a SOC below the threshold. In addition, it will assign some of these DEVs to the dedicated charging service to charge. During matching, the different numbers of DEVs and charging services can result in one of three possible states: (a) DEVs greater than charging services, (b) DEVs equal to charging services, and (c) DEVs smaller than charging services. Here, we take into account every possibility. In the following sections, our method for allocating DEVs to the random and dedicated charging services will be demonstrated. The DEVs then go to the associated charging service place for mutual charging when the central RSU has transmitted the pair-matching findings to the DEVs and charging services. For the lowest cost of the entire system or to fulfill the special advantage of charging services or DEVs, it is feasible

to match charging services and demanding charge EVs. Here, we examine the minimum charging cost of DEVs.

As previously mentioned, our system involves multiple zones with intersections. These zones can collaborate to optimize the number of matched EVs across all areas. Since the fog nodes of different zones are interconnected, when a DEV sends its charging request to a zone, the corresponding fog node can communicate with adjacent zone fog nodes. This communication aims to identify available charging services, including unused SEVs and unused MCSs that can move to the zone to function as additional SEVs or MCSs if possible. Essentially, depending on the proximity, a zone can use charging services from other zones to maximize the total number of charged EVs. Figure 3.2 shows the interaction of the EVs and charging services with the fog services of the current zone and the nearby zones.

3.2 Problem Formulation

In this section, we present the cost and utility of the participating parties in the proposed model. We extend some of the mathematical models presented in [3], [6], and [15]. This work focuses on fog-based development. Hence, it does not consider the integration of multiple zones or a cloud system for integration of multiple zones.

In each zone, let $J = \{1, 2, ..., f\}$ represents the set of DEVs, and the sets $K = \{1, 2, ..., g\}$, $I = \{1, 2, ..., w\}$, $H = \{1, 2, ..., x\}$, and $M = \{1, 2, ..., y\}$ represent the SEVs, FCSs, HCSs, and MCSs charging services of the zone respectively. In addition, we consider the set of MPs as $L = \{1, 2, ..., o\}$. In the following, we will outline a method for prioritizing DEVs based on their maximum travel distance capabilities. Furthermore, we formulate the cost of charging DEVs by the available charging services and the utility derived from each specific charging service.

3.2.1 Prioritizing DEVs

In this section, we prioritize the DEVs based on the maximum distance they can travel with their current SOC (soc_j^c). This distance is defined as:

$$d_j^{th} = (soc_j^c - \Gamma)\, d_j^{predicted} \tag{3.1}$$

where $d_j^{predicted}$ presents the predicted range or distance DEV j can cover in a single charge (in km). In our system model, we assume that RSUs serve as fog nodes embedded

within ABB software are equipped with ML capabilities. This enables them to predict this parameter by considering a range of influencing factors. As an illustration of this predictive capability, we have developed an ensemble-based robust ML aimed at precisely predicting the driving range of EVs, harnessing big data. Further details regarding the development of this model will be elaborated in Chapter 4.

(Γ) is the threshold that DEVs stay above before it enters into range anxiety. In our mechanism, the DEV with the lowest d_j^{th} is given the highest priority among all the DEVs when allocating charging services.

3.2.2 Cost model formulation

In this section, the charging cost of each service is discussed in detail.

- Cost of charging DEV j with SEV k at location $l \in L$:

  In our model, both DEV j and SEV k should meet each other to complete the charging process. The cost of charging DEV j with SEV k is denoted by $c_{j,l}$ and is defined as:

  $$c_{j,l} = p_k \, q_j + c_{j,l}^t + c_j^{ti} + c_j^s \tag{3.2}$$

  where p_k is the energy unit price determined by SEV k, and q_j denotes the quantity of energy required by DEV j to reach its desired SOC, as determined by the following calculation:

  $$q_j = soc_j^r \; b_j^c \tag{3.3}$$

  Here soc_j^r is the percentage of the required state of charge for DEV j, and b_j^c is the battery capacity (in kWh) of DEV $j \in J$. In (3.2), $c_{j,l}^t$ is the cost of energy for DEV j to travel from its current location to the meeting point l to obtain energy from SEV k. The following formula presents its calculation:

  $$c_{j,l}^t = p_0 \, d_{j,l} \, c_j^e \tag{3.4}$$

  where c_j^e is the cost of energy consumption per kilometer (in kWh/km) of DEV j. In our system model, RSUs function as fog nodes equipped with machine-learning capabilities to predict energy consumption based on various influencing factors. It is expected that EV owners will charge their vehicles at home at a low cost, therefore, p_0 is the original unit energy price for EVs. Additionally, the available SOC for each SEV k is soc_k^a. To simplify the analysis, we assume that all SEVs are fully charged when they are ready to supply the DEVs. Therefore, soc_k^a is calculated as the difference between the initial SOC (100%) and the required

SOC for subsequent trips after completing the charging process. $d_{j,l}$ is the distance between DEV j and ML l. The cost of time for DEV j (c_j^{ti}) is calculated by adding the driving time, charge duration time, and additional waiting time (t_j^w), and then multiplying the result by the parameter α as value of time. For simplicity, we assume that the value of time is the same for both DEVs and SEVs. The driving time is the duration required for the EV to move from its current location to the ML, while the charge duration time represents the time taken for the EV to exchange energy during the charging process.

$$c_j^{ti} = \alpha \, (d_{j,l}/v_j + q_j/\lambda \, r^e + t_j^w + t_j^{idle}) \tag{3.5}$$

Here, v_j represents the average speed of DEV j determined prior to executing the matching algorithm, utilizing the speed limit on streets without traffic, while t_j^{idle} denotes the idling time DEV j spends in traffic while traveling to the charging location. λ expresses the ratio of actual energy transferred to total energy required, also known as the V2V energy transfer efficiency. r^e (in kW), which is the same for DEVs and SEVs, is the rate of energy exchange per unit of time. It is relying on the bidirectional connector of the V2V energy exchange.

DEVs assigned to charging services will be charged according to their priority. In situations where the charging location capacity is limited, certain DEVs within a charging location may need to wait for others with higher priority to complete their charging process. It imposes t_j^w as an additional waiting time for DEV j. Assume that DEV j at the designated charging location needs to wait for Z other DEVs to complete charging. Under this assumption, the formula representing the cost associated with the waiting time of DEV j at the charging location expresses as follows:

$$t_j^w = \sum_{z=1}^{Z} (q_z/\lambda \, r^e) \tag{3.6}$$

where q_z denotes the amount of energy requested by DEV z for charging prior to DEV j.

In (3.2), c_j^s is an additional cost imposed on the DEV to compensate for the cost of SEVs traveling to MLs to charge DEVs. It is defined as follows:

$$c_j^s = c_{k,l}^t + c_k^{ti} + c_k^b \tag{3.7}$$

where $c_{k,l}^t$ is the cost of energy for SEV k to travel to the ML l from its current location, given as follows:

$$c_{k,l}^t = p_0 \, d_{k,l} \, c_k^e \tag{3.8}$$

Here c_k^e is the cost of energy consumption per kilometer (in kWh/km) for SEV k. In (3.7), c_k^{ti} is the cost of time for SEV k determined by the following equation:

$$c_k^{ti} = \alpha \left(d_{k,l}/v_k + q_j/\lambda \, r^e + t_k^{idle} \right) \tag{3.9}$$

where v_k is average speed of SEV k calculated before initiating the matching algorithm, utilizing the street speed limits in the absence of traffic, whereas t_k^{idle} denotes the time SEV k remains stationary in traffic while en route to the charging location. $d_{k,l}$ is SEV k and ML l distance. In (3.7), c_k^b shows the cost of battery degradation for the SEV k as a result of discharging to the DEV j and is given as follows:

$$c_k^b = c^r \, \theta \, q_j \tag{3.10}$$

where c^r and θ are the cost of replacing the battery and the coefficient of battery capacity degradation, respectively.

- Cost of charging DEV j with HCS h or FCS i:

  FCSs and HCSs are other available charging services for charging DEV j. The total cost to the DEV j of getting energy through FCS i is $c_{j,i}$ and through HCS h is $c_{j,h}$ as follow:

$$c_{j,h} = p_h \, q_j + p_0 \, d_{j,h} \, c_j^e + c_j^{ti} \tag{3.11}$$

$$c_{j,i} = p_i \, q_j + p_0 \, d_{j,i} \, c_j^e + c_j^{ti} \tag{3.12}$$

  where p_i and p_h denote unit energy trading price determined by FCS i and HCS h, respectively. $d_{j,i}$ and $d_{j,h}$ are the distance between DEV j and FCS i, and between DEV j and HCS h, respectively.

- Cost of charging DEV j with MCS m:

  Our model considers MCSs as another available charging service so that MCS m can charge up DEV j with the following cost:

$$c_{j,m} = p_m \, q_j + p_0 \, d_{j,m} \, c_j^e + c_j^{ti} + c_m^b \tag{3.13}$$

  It is noteworthy that for MCSs, the waiting time for DEVs (t_j^w in c_j^{ti} in (5)) is usually considered zero in simulations because DEVs arriving at the predetermined meeting locations can access charging services immediately without waiting, thanks to the organized nature of MCS operations. Here p_m denotes the energy unit price determined by MCS m, and c_m^b signifies the cost of battery degradation of MCS

m given as follows:

$$c_m^b = c^r \, \theta \, q_j \tag{3.14}$$

The final cost of charging DEVs using available charging services is the summation of $c_{j,l}$, $c_{j,i}$, $c_{j,h}$, and $c_{j,m}$.

3.2.3 Charging services utility

The utility acquired by any charging service (SEVs, FCSs, HCSs, and MCSs) for supplying charging to DEVs is given as follows:

$$u_j^{ch} = p \, q_j - p_0 \, q_j / \lambda \tag{3.15}$$

where $p = p_k$ for SEV k, $p = p_h$ for HCS h, $p = p_i$ for FCS i, and $p = p_m$ for MCS m.

3.3 Summary

This chapter illustrates our proposed system model and problem formulation, presenting the formulas for the cost and utility of participants in our matching algorithm deployed within the system model. Additionally, it introduces the formula for prioritizing DEVs as a part of the initial step of our matching algorithm, which is based on the maximum distance DEVs can travel with their current SoC. To enhance the accuracy of this prioritization, we have developed an ML-based method to predict this distance based on several influencing factors. The subsequent chapter will delve into this range prediction and provide the prediction results. Following that, in Chapter 5, we detail the proposed Maximum Capacity-Based Cooperative Algorithm, which is based on the aforementioned formulas introduced in this chapter.

Chapter 4

Driving Range Estimation with Ensembled ML Model

The main objective of this chapter is to develop a predictive ML model for EV driving range prediction, addressing a non-sequential regression problem. To ensure the robustness and reliability of our estimation model, we undertake a series of crucial statistical procedures, including data cleaning, scaling, and Exploratory Data Analysis (EDA). This integration of ML techniques for precise EV range prediction will play a pivotal role in prioritizing DEVs in Equation 3.1 in Chapter 3 as part of the initial steps of our proposed matching algorithm. Further details on the algorithm will be provided in the subsequent chapter.

4.1 Methodology

This section outlines our methodology, which involves several ML models, each undergoing a seven-phase process: data collection, initial data preprocessing, EDA, final data preprocessing, feature engineering, K-fold CV, and model implementation for prediction. Fig. 4.1 illustrates these phases. Following this methodology for each model, we record and compare the results for both CV and prediction. Subsequently, we select the model that yields the best results.

The proposed framework encompasses distinct phases, commencing with the data collection phase, where we offer a comprehensive overview of the dataset under investigation. Subsequently, through EDA, we diligently address issues, like missing values, removal of outliers, and feature dimensionality reduction. During the EDA step, we conduct final data analysis using plots and statistical methods to inform subsequent phases. Encoding

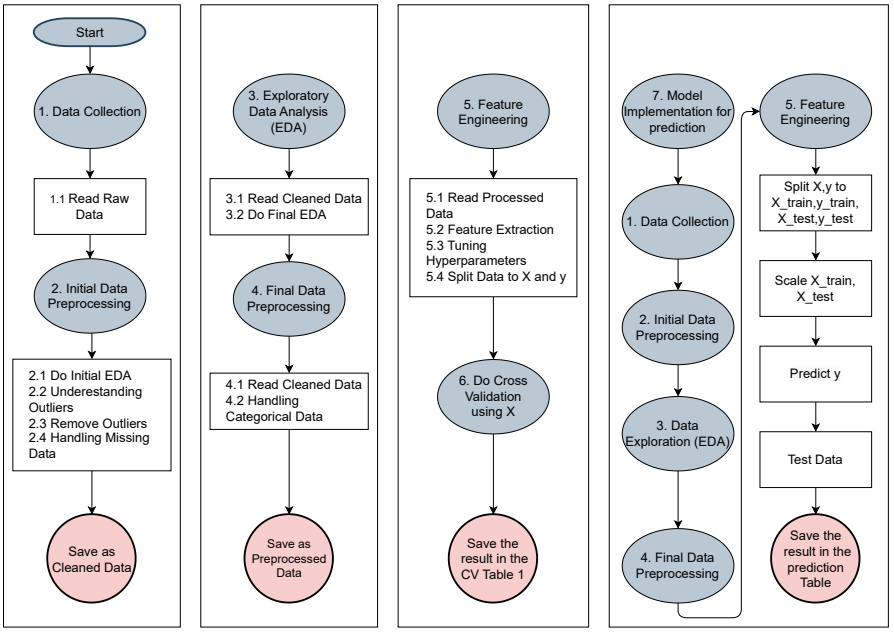

FIGURE 4.1: Flowchart illustrating the methodology of the applied ML model.

categorical data is performed in the final preprocessing phase followed by the feature engineering phase, where we extract optimal features. Moving on to the CV phase, our approach involves the unimodal building and evaluation, considering various ML models, say, Extreme Learning Model (ELM), XGBoost, MLR, Multilayer Perceptron (MLP), deep MLP, RF, AdaBoost, and SVR; through K-fold CV. Subsequently, in the model implementation phase, we exploit the two best models for generalized model building under an ensemble architecture.

4.1.1 Data Collection

Data plays a pivotal role in the field of predictive modeling. To examine the variables influencing the driving range in real-world EV scenarios, we have utilized a dataset encompassing twenty attributes as tabulated in Table 4.1. This benchmark dataset is obtained from the authentic source https://www.spritmonitor.de.

4.1.2 Initial Data Preprocessing

The original dataset necessitated comprehensive preprocessing due to the presence of irrelevant information and missing values, making it a crucial initial step in our analysis. During this phase, we systematically remove irrelevant features those lacking any predictive value for range estimation. The attributes that are removed before model building are as follows: `manufacturer`, `odometer`, `version`, `fuel_date`, `fuel_note, model`,

TABLE 4.1: The attributes influencing the remaining range of EVs

Attributes	Description
Input Variables	
`manufacturer`	The company or brand that produced the EV
`model`	The specific make and model of the EV
`version`	A particular variant or edition of the EV model
`power(kW)`	The maximum power output that the motor can deliver under normal operating conditions in kW
`fuel_date`	The date on which the EV was fueled or charged
`odometer`	The total distance that the EV has traveled since its initial use or since the last reset
`quantity(kWh)`	The total amount of energy consumed by an EV in kWh
`fuel_type`	The type of energy or fuel used to power the EV, which in this case is electricity
`tire_type`	The type of tires used on the EV, which in this case are winter, summer, and all-year tires
`city`	If EV drives in the city or not
`motorway`	If EV drives in the Motorway or not
`country_roads`	If EV drives in the Country Roads or not
`driving_style`	The manner in which the EV is driven, which in this case are normal, moderate, and fast
`consumption(kWh/100km)`	The rate of energy consumption of EV in kWh per 100 kilometers. It represents energy efficiency
`A/C`	The use of air conditioning within the EV, which can impact energy usage
`park_heating`	The use of the heating system of the vehicle
`avg_Speed (km/h)`	The average speed at which the EV is driven in km/h
`ecr_deviation`	The Difference between the energy consumption rate recorded and the value announced by the manufacturer
`fuel_note`	Additional notes or comments related to the EV's fueling, charging, or performance
Target Variable	
`trip_distance(km)`	The range or distance that the EV can travel on a single charge in Km

`fuel_type`, and `ecr_deviation`. It's important to note that we retain the `power(kW)` feature as it provides valuable information about various EV models in our dataset. Addressing missing values involves a combination of removal and imputation. To handle missing values in the `avg_speed (km/h)` that has the highest number of gaps, we employ the alpha trim mean with $\alpha = 0.1$. Simultaneously, we remove rows with missing values in other features.

Additionally, this phase involves the identification and treatment of outliers, which are data points significantly deviating from the majority and capable of skewing statistical analyses. An initial EDA is conducted to gain insights into outliers for the features `trip_distance(km)`, `quantity(kWh)`, `consumption(kWh/100km)`, and `avg_speed(km/h)`. For the removal of outliers, we employed the interquartile range (IQR) method alongside a specific outlier removal strategy based on the EDA results. The analysis indicated that removing outliers based on EDA yielded superior results. Fig. 4.2 presents the initial EDA for the mentioned features. As seen in our EDA analysis, data values exceeding 650 for `trip_distance(km)`, 110 for `quantity(kWh)`, 70 for `consumption(kWh/100km)`, and 100 for `avg_speed(km/h)` were considered outliers. Consequently, we systematically

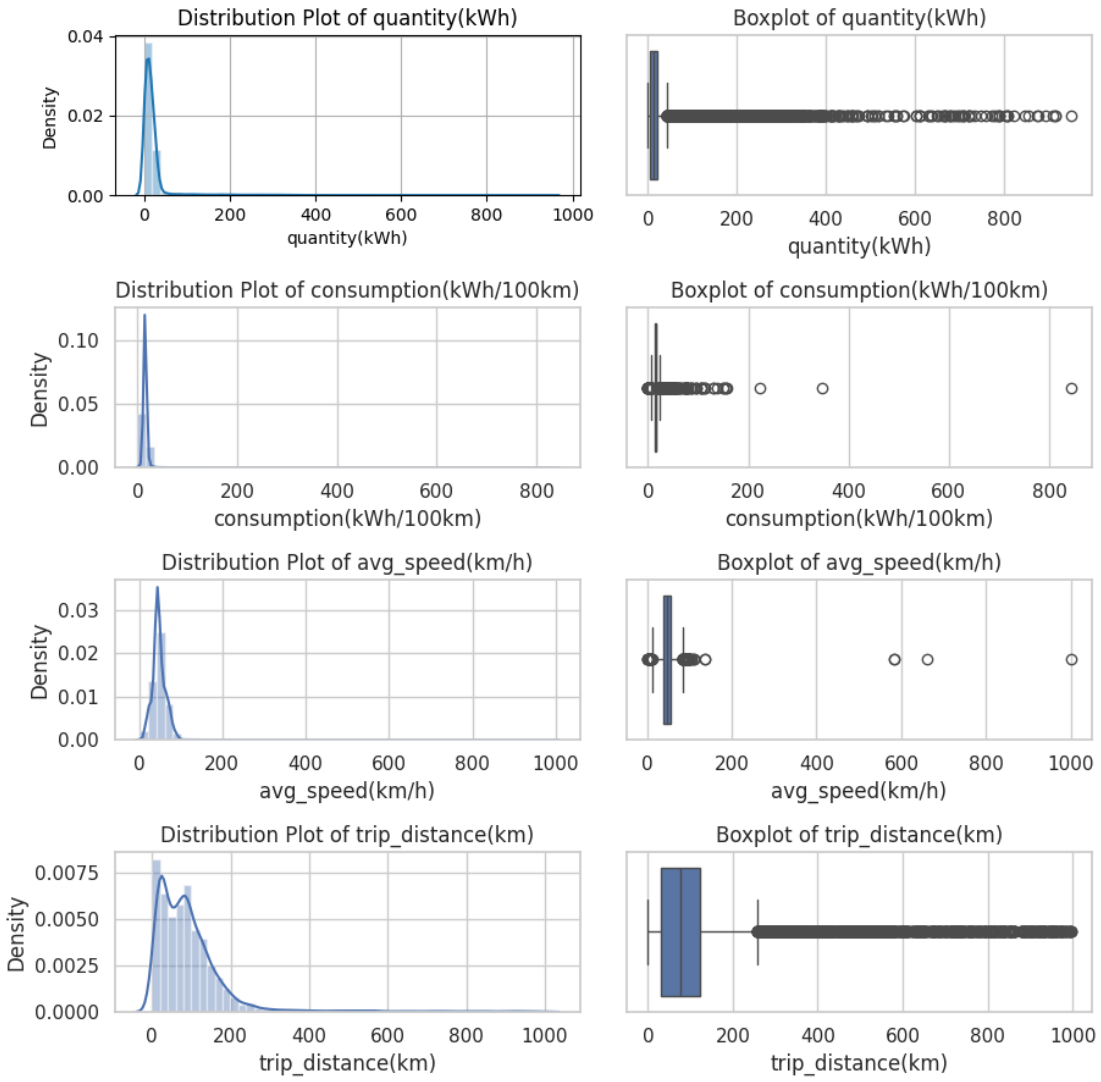

FIGURE 4.2: EDA for gain insights into outliers for trip_distance(km), quantity(kWh), consumption(kWh/100km), and avg_speed(km/h) Features.

removed all these outliers from our dataset. The cleaned data was then saved as a CSV file for further analysis.

4.1.3 Exploratory Data Analysis

We conduct comprehensive EDA encompassing univariate, bivariate, and multivariate analysis. It involves understanding data distribution and characteristics, identifying insignificant features, and selecting an optimal number of information-rich features. This phase serves as a crucial preparatory step for the subsequent phases, namely feature

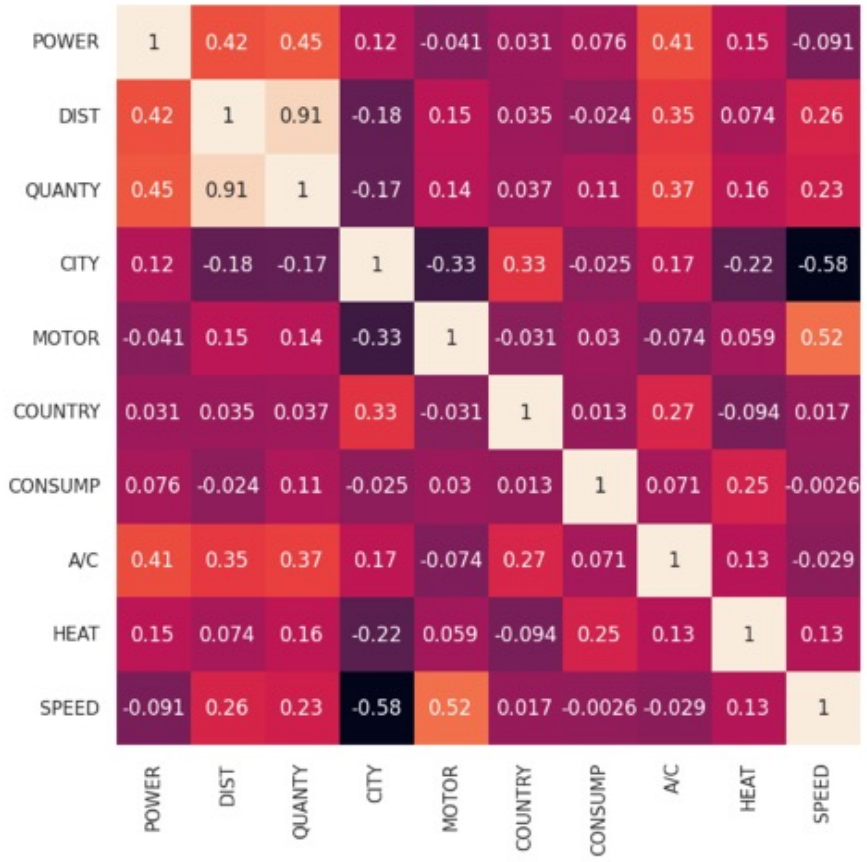

FIGURE 4.3: Heatmap illustrating the correlation structure of the cleaned dataset. Legend: `POWER - power(kW)`, `DIST - trip_distance(km)`, `QUANTY - quantity(kWh)`, `CITY - city`, `MOTOR - motor_way`, `COUNTRY - country_roads`, `CONSUMP - consumption(kWh/100km)`, `A/C - A/C`, `HEAT - park_heating`, and `SPEED - avg_speed(km/h)`.

engineering and model building. For multivariate EDA, we employ data correlation analysis on the cleaned data as illustrated via a heat map visualization shown in Fig. 4.3.

4.1.4 Feature Engineering

In real-world conditions, the driving range of EVs is influenced by a multitude of factors. To mitigate overfitting, a limited set of features that do not increase the complexity of the model is required. Consequently, a feature engineering process is crucial to further identify the irrelevant attributes from the input set created after the initial data pre-processing phase (cf. Section 4.1.2). Thus, we conduct two dimensionality reduction techniques using Correlation Analysis (CA) and Principal Component Analysis (PCA). The sanity analysis conducted using these methods shows that the models built CA-based feature engineering achieve the best performances.

TABLE 4.2: Ten-Fold CV results of various ML models considered in this study using the entire dataset. The best performance is inked in blue.

Model	Average MAE	Best MAE	Average R2	Best R2
ELM	12.357	11.818	0.894	0.909
XGBoost	12.373	11.872	0.904	0.918
MLR	16.628	16.035	0.853	0.868
MLP	12.635	12.046	0.901	0.913
Deep MLP	13.182	12.191	0.898	0.911
RF	10.274	9.816	0.919	0.931
AdaBoost	16.001	15.600	0.880	0.896
SVR	19.224	18.817	0.773	0.782

In the case of PCA technique, performance improvements vary across different ML models and with the number of principal components used in the PCA method. We initiated with a smaller number of components and gradually increased them while monitoring model performance. Ultimately, the best performance for PCA technique was achieved with ten principal components. However, it's noteworthy that the outcomes of CA analysis surpassed those of PCA method in both ten-fold CV and the final implementation of ML models. Detailed results of ten-fold CV and the final model implementation for PCA technique can be found in Appendix A.

Regarding CA technique, it was noted that `tire_type` exhibits no significant correlation with the target variable, `trip_distance(km)`. Hence, we opted to eliminate this feature from consideration.

4.1.5 Cross-Validation

The models' hyperparameter tuning is conducted through CV grid search, systematically. This process enhances the models' performances, ensuring optimal parameter selection to mitigate overfitting. The resulting hyperparameters are detailed in Table 4.3. Subsequently, we assess the predictive performance of the tuned models through comprehensive experiments and standard statistical evaluation metrics, such as the R2 score and MAE. The formulas for these metrics are detailed in Chapter 2.1 in Equations 2 and 2. For the convenience of the reader, we reproduce these formulas here.

These metrics provide valuable insights into the model's robustness. For a given n number of observations with y_i representing the i-th instance of actual values of the target variable, $\hat{y}_i$ denoting the i-th instance of predicted values of the target variable, and $\bar{y}$ representing the mean of the actual values, the R2 score is calculated as in (4.1), while MAE is computed as in (4.2).

TABLE 4.3: Optimized values of the hyperparameters of various models used in this work after CV-based grid search and fine tuning

Model	Hyperparameters
ELM	`activation= 'tanh',hidden_layer_sizes=(150,), alpha=0.01`
XGB	`n_estimators=100, learning_rate=0.15, max_depth=3`
MLR	-
MLP	`hidden_layer_sizes=(100,), max_iter=1000, n_iter_no_change=100, activation='relu',alpha= 0.01, solver='adam'`
Deep MLP	`activation='relu',alpha=0.01, hidden_layer_sizes=(100, 50,13,7), learning_rate='constant',solver='adam'`
RF	`n_estimators=250, max_depth=10, min_samples_split=5, min_samples_leaf=2`
AdaBoost	`n_estimators=200, learning_rate=0.01, loss='exponential'`
SVR	`C=1, epsilon=0.5, kernel='rbf'`

$$R^2 = 1 - \frac{\sum_{i=1}^{n}(y_i - \hat{y}_i)^2}{\sum_{i=1}^{n}(y_i - \bar{y})^2}, \tag{4.1}$$

$$MAE = \frac{1}{n}\sum_{i=1}^{n}|y_i - \hat{y}_i| \tag{4.2}$$

We employ K-Fold CV for model evaluation, where the K is set to ten. The overall performance of the model is calculated as the average across the ten iterations using the entire dataset.

4.1.6 Final Predictive Model Implementation

In this phase, we choose the best models based on the K-Fold CV analysis given in Table 4.2, for building stronger predictive models, including the ensemble-based strategy using single mutually exclusive training (70%) and a hold-out (30%) sets created from the dataset. The ensemble architecture exploits RF, XGBoost, MLR, and MLP in combination with two models. Notably, for models, such as MLR, MLP, and Deep MLP, we apply feature scaling to enhance their performance. These models benefit from scaling to ensure uniformity in the impact of different features on the learning process.

4.2 Experimental Results and Analysis

From Table 4.4, it is observed that the deep MLP model achieves the highest performance without encountering overfitting issues. MLR, on the other hand, exhibits a minimal

TABLE 4.4: Quantitative analysis of the final models built using single training and hold-out sets and their performances. The best performances on the hold-out set are inked in blue.

Model	Training MAE	Test MAE	Training R2	Test R2	Inference Time (s)
ELM	12.195	12.649	0.894	0.888	57.2126
XGBoost	11.721	12.710	0.910	0.892	4.07593
MLR	16.259	16.490	0.855	0.832	3.97173
MLP	11.022	11.131	0.913	0.902	77.4339
Deep MLP	9.430	11.738	0.926	0.921	29.1965
RF	7.903	10.698	0.954	0.908	8.63254
AdaBoost	14.45	15.155	0.889	0.877	10.6481
RF and XGBoost	8.118	10.459	0.951	0.916	33.3540
MLR and XGBoost	11.759	12.656	0.905	0.909	9.69264
RF and MLP	8.691	9.5100	0.944	0.935	494.764

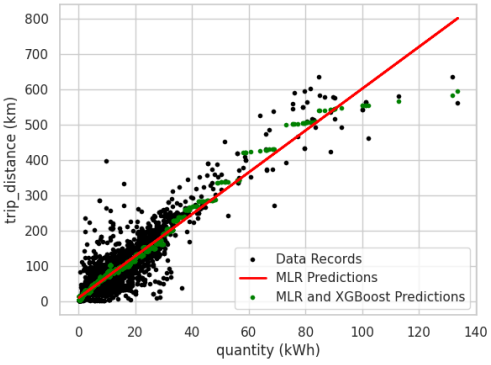

((a)) Driving range based on quantity applying MLR (R2 score=0.832) and ensembled model using MLR and XGBoost (R2 score=0.909)

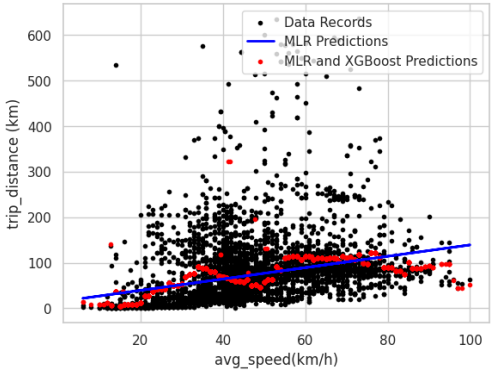

((b)) Driving range based on average speed applying MLR (R2 score=0.832) and ensembled model using MLR and XGBoost (R2 score=0.909)

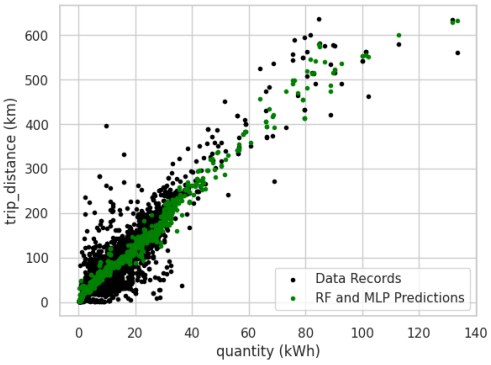

((c)) Driving range based on quantity applying ensembled model using RF and MLP (R2 score=0.935)

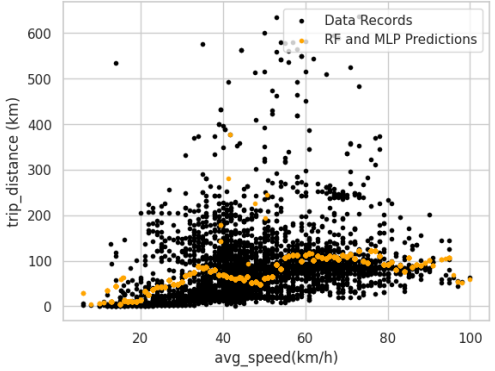

((d)) Driving range based on average speed applying ensembled model using RF and MLP (R2 score=0.935)

FIGURE 4.4: Comparison between prediction and actual driving range wrt quantity and average speed. Note that the input is a multidimensional data. So, for visualization purposes, the plots consider a single attribute on the horizontal axis.

inference time of $\approx$ 4 seconds. Similar to deep MLP, the RF model also records a relatively good performance; however, there are discernible signs of overfitting. To address this overfitting concern and enhance the accuracy of the predictions, we utilize the ensemble technique by leveraging the strengths of the best individual models. For instance, the integration of the RF with XGBoost, RF with MLP, as well as MLR with XGBoost yielded noticeable improvements. Hence, the ensemble model with RF and XGBoost still seems to experience overfitting to some extent, but the ensemble model with RF and MLP considerably resolves the issue with compromising the inference speed. On the other hand, the ensemble of MLR and XGBoost results in increased prediction to an R2 score of 0.91 without facing overfitting issues compared to the uni-modal MLR, with a reasonable inference time. Therefore, we identify this model as the best choice for an accurate driving range estimation. Fig. 4.4(a) compares the predictive performances of the unimodal MLR and the ensemble model using MLR and XGBoost. For simplicity of visualization purposes, the plots are drawn based on the consumed energy amount (`quantity (kWh)`). Similarly, Fig. 4.4(b) presents another fitted line generated exclusively from the average speed value (`avg_speed`). Notably, a substantial correlation between the quantity and the driving range is evident. However, this correlation is less pronounced when considering the average speed. Fig. 4.4(c) showcases the results of the ensemble model using RF and MLP based on the total energy consumed (`quantity (kWh)`). Similarly, Fig. 4.4(d) portrays the model's performance wrt the average speed (`avg_speed`).

4.3 Summary

In this chapter, we provide a detailed overview of our ensemble-based ML model designed for accurately predicting the range of EVs. This prediction played a crucial role in the preceding chapter, where it was utilized for prioritizing DEVs as part of the initial step of our proposed matching algorithm. The algorithm itself will be comprehensively elucidated in the subsequent chapter.

Chapter 5

Cooperative Fog-Based En-route EV Charging Services

In this chapter, we outline the development of the proposed matching algorithm, which aims to foster collaboration among various charging services, including SEVs, FCSs, HCSs, and MCSs, to optimize the charging process for DEVs. The algorithm introduces a strategic approach to address practical scenarios based on the number of DEVs and available charging services within each zone, as elaborated in Section 5.1. Furthermore, in section 5.2, we present the evaluation results of our algorithm based on some performance measurements and we will compare the results of our proposed matching algorithm to an existing study which utilizes Gale-Shapley game based matching algorithm.

5.1 Maximum capacity-based cooperative Algorithm

This section proposes a cooperative matching technique based on the Hungarian algorithm called the maximum capacity-based cooperative algorithm. The subsequent subsections detail the step-by-step procedure of the algorithm for each zone, as depicted in Algorithm 3.

5.1.1 Initial assignment of DEVs to charging locations

This subsection presents a detailed explanation of steps 1 to 4 of Algorithm 1. During the first step, the corresponding fog node determines the count of DEVs within each zone and the availability of charging services. If the available charging services are insufficient

to accommodate the DEVs, the fog node proceeds to communicate with adjacent zones. This helps to see if they have available unused MCSs/SEVs interested in moving toward the desired zone. To optimize cost efficiency, the distance between MCSs/SEVs and the zone must not be farther than a threshold parameter, δ. The parameter δ is calculated to be less than half the dimension of the zone, preventing excessive charging costs and ensuring that the MCSs/SEVs are within a reasonable proximity to the target zone. Thereafter, the fog node asks for notification from the nearby zones if such charging services are accessible, adding them to the charging services. Based on this information, the algorithm indicates f as the final number of DEVs and n as the total number of charging services available. According to equation (3.1), in step 2, the d_j^{th} values of all DEVs are calculated. The DEVs are prioritized accordingly, that is, the lower the value the more priority DEV has. Furthermore, the algorithm calculates the distances between all DEVs and all charging locations, as well as the distances between all SEVs and all MPs. The algorithm then, in step 3, selects those MPs, FCSs, HCSs, and MCSs locations with a distance less than d_j^{th}. Going to step 4, among the selected charging locations from step 3, each DEV is initially assigned to the charging location that has the minimum distance with respect to the DEV. Next, in step 5, we consider three aforementioned states for our system model as (a) DEVs number $<$ charging services number, (b) DEVs number $=$ charging services number, and (c) DEVs number $>$ charging services number.

5.1.2 Implementation of states (a) and (b)

In states (a) and (b), there are sufficient charging services to charge all DEVs. Following step 5.1, depending on the number of DEVs and charging locations, the ideal number of DEVs that each charging location should accommodate is calculated under the two following conditions: 1- No charging location is left without assigned DEVs, and 2- The allocation of DEVs to each charging location is maximized. Based on these conditions, if a charging location has excess DEVs, the algorithm proactively reassigns the DEVs with lower priorities to the available unused charging locations with the shortest distance to them.

For example, assume we have 5 DEVs and 7 charging locations, ideally accommodating 1 DEV each. Initially, we allocated these 5 DEVs to the charging locations based on the minimum distance criterion in step 4. As a result, 3 DEVs were assigned to the first location, 1 to the second, and 1 to the seventh, leaving locations 3rd-6th unallocated. Consequently, the 3 DEVs at the first location must wait for their turn to charge, while the empty locations could have been utilized to charge them promptly. To resolve this, 2 DEVs with a lower priority from the first location are reassigned to charging locations 3rd to 6th, which are closest to them. This final assignment ensures

each location accommodates only 1 DEV, minimizing waiting time, and optimizing the charging process.

In the subsequent step 5.2 of the algorithm, if DEVs are assigned to MPs, the charging cost is calculated, followed by the utilization of the Hungarian algorithm to pair them with SEVs. Consequently, the paired DEVs and SEVs travel to the designated MPs to initiate the charging process, following their assigned priorities. On the other hand, if the DEVs are allocated to the FCSs, HCSs, and MCSs locations, the algorithm calculates the cost of charging for each DEV. Subsequently, the DEVs proceed toward the charging locations for being charged given their priorities.

5.1.3 Implementation of state (c)

In state (c), the available charging services are insufficient to accommodate all the DEVs. To address this situation, we assume that some SEVs, such as the Ford F-150 Lightning, possess a considerable battery capacity, enabling them to charge more than one DEV. Consequently, our algorithm is designed to allow each SEV k, with the available state of charge soc_k^a, to charge the maximum number of DEVs. To achieve this, we introduce a parameter, defined as $Itr = \lceil \frac{f}{n} \rceil$, ($f$ represents the number of DEVs, while n represents the number of available charging services). The parameter Itr is formulated to accommodate a specific scenario where the number of DEVs and available charging services remains relatively constant within a limited time frame. We have defined this time frame by restricting Itr as the iteration number for directing DEVs toward charging services without updating the number of DEVs and charging services. After the designated iterations, the algorithm can be re-executed with updated values of f and n, allowing for dynamic adjustment to any changes in the system's parameters. This framework allows us to explore how our algorithm can efficiently manage DEV charging within a constrained time frame, as indicated by Itr=3. Additionally, by setting 'Itr' to a value no larger than 3, we aim to prevent a significant increase in the waiting time of DEVs, as this ensures that the algorithm adapts to the initial conditions without excessively prolonging the charging process. If Itr exceeds 3, the algorithm restricts its value to 3 and returns to steps 5.4 to 5.10 for further processing. As a result, the algorithm for the state (c) has two possible values for Itr: $Itr = 2$ and $Itr = 3$.

During step 5.4, if the number of DEVs assigned to each FCS, HCS, and MCS location in step 4, is not equal to $Itr - 1$, the algorithm proceeds to reassign DEVs to each FCS, HCS, and MCS location to ensure that each of these charging locations accommodates $Itr - 1$ DEVs. In step 5.5 of the algorithm, we focus on the DEVs that have not been assigned to FCSs, HCSs, and MCSs locations in step 5.4. From this set of DEVs, we

need to create a group of DEVs whose size matches the number of available SEVs to be paired with. This group is formed as the first priority for matching with SEVs. With this objective in mind, we conducted a comparison between two groups of DEVs, the first group with a higher q_j value and the second group with a lower q_j value. we, then, run our algorithm with the groups to get the results of the rate of charged DEVs. Represented in Figure 5.1, the curves show that grouping DEVs with a greater value of q_j leads to more numbers of charged DEVs. For this reason, we adopt the algorithm in a way that an equal number of DEVs with SEVs demanding higher q_j values are chosen. At present, an equal number of DEVs and SEVs are available for mutual charging on MPs. In step 5.6 of the algorithm, if the MPs designated to accommodate the group of DEVs created in step 5.5 are assigned to more than one DEV, any excess number of DEVs at the MPs with lower priority will be reallocated to other MPs that have the minimum distance to those DEVs. This reallocation guarantees that DEVs can be charged promptly and efficiently, avoiding any unnecessary waiting time. The following description outlines the process for all cycles of sending DEVs toward charging services, 2 cycles when $Itr = 2$ and 3 cycles when $Itr = 3$.

- **First Cycle:** During the first cycle of sending DEVs to charging services, in step 5.7 of the algorithm, the matching process is performed by determining the charging costs of pairing the grouped DEVs (from step 5.5) with SEVs. The algorithm calculates the charging costs associated with each possible combination of DEVs and SEVs. Subsequently, the Hungarian algorithm is utilized to optimally match the DEVs with the available SEVs based on the calculated charging costs. Once the pairing is complete, the DEVs and SEVs are directed toward the MPs to commence the charging process. In parallel, among the DEVs assigned to FCSs, HCSs, and MCSs locations, the algorithm calculates the charging cost for one DEV at each charging location with higher priority. These DEVs then proceed to their respective charging locations to initiate the charging process.

- **Second Cycle:** Following the aforementioned steps, there are still some DEVs that remain uncharged. In order to address this, during steps 5.8 and 5.9, the unmatched DEVs are identified, and the new SOC value for the SEVs is computed. When $Itr = 2$, during the second cycle as the final step of the matching algorithm, step 5.10.1 involves the computation of costs of charging unmatched DEVs with all the available charging services. Subsequently, during steps 5.10.2 and 5.10.3, the unmatched DEVs are paired with charging services using the Hungarian method, aiming to minimize the total cost of the DEVs. In step 5.10.4, the matched DEVs proceed toward the assigned charging services to undergo the charging process.

During the second cycle of the charging process when $Itr = 3$, step 5.10.5 addresses the unmatched DEVs that have not been assigned to FCSs, HCSs, and MCSs locations. For these unmatched DEVs, the algorithm calculates the charging costs associated with pairing them with SEVs that have a new SOC due to the first cycle charging. Accordingly, Using the Hungarian Algorithm, the algorithm attempts to optimally match a specific number of these unmatched DEVs with SEVs, allowing them to travel to the location of the SEVs for charging. This step ensures efficient utilization of SEVs to support the charging process for the remaining unmatched DEVs. Simultaneously, the algorithm calculates the charging costs for other unmatched DEVs that have been assigned to each FCS, HCS, and MCS location in step 5.4. These DEVs, now having a lower priority, proceed to their respective charging locations for charging.

- **Third Cycle:** During the third cycle for $Itr = 3$, steps 5.8, 5.9, and 5.10.1 to 5.10.4 are repeated to address the remaining uncharged DEVs.

The flowchart illustrating the algorithm can be found in Figure 5.2.

5.1.4 Computational Complexity

The proposed algorithm consists of several loops that iterate over sets of DEVs, SEVs, charging services, and main charging locations, with sizes denoted by f, g, w, x, y, and b, respectively. Additionally, the steps involving distance calculations, charging costs, and SOC computations for DEVs and SEVs involve linear-time operations based on the sizes of the respective sets. The Hungarian algorithm used in Step 5.2.3 has a time complexity of approximately $O(n^3)$, where n is the number of DEVs and SEVs being matched. Overall, the algorithm is expected to have a $O(n^3)$ complexity of the Hungarian algorithm used for assignment.

5.2 Simulation and Numerical Results

This section discusses the evaluation of the proposed model and the simulation results.

5.2.1 Simulation Parameters

In this study, we conducted a case study involving the simulation of a network of DEVs and charging services within the Thunder Bay area. The area was segmented into three zones: top, middle, and bottom. The locations of existing FCSs within the area

Algorithm 3 Maximum capacity-based cooperative Algorithm

Inputs :
1. Set of DEVs $J = \{1, 2, ..., f\}$, set of charging services including $K = \{1, 2, ..., g\}$, $I = \{1, 2, ..., w\}$, $H = \{1, 2, ..., x\}$, and $M = \{1, 2, ..., y\}$, and set of MPs L=$\{1, 2, ..., b\}$.
2. Initial Parameters includes p_0, α, r^e, λ, c^r, θ, and Γ.
3. The dataset includes b_j^c (kwh) and c_j^e (kwh/km) of EVs.
4. Location of FCSs, HCSs, MCSs, SEVs, MPs, and DEVs.
5. soc_j^c and soc_j^r of DEVs and soc_k^a of SEVs.

Steps :
1.1. **for** *each unused SEV in adjacent zones* **do**
  if *Distance between SEV and current zone*$< \delta$ **then**
    $K = \{1, 2, ..., g+1\} \leftarrow K = \{1, 2, ..., g\}$
  end if
end for
for *each unused MCS in adjacent zones* **do**
  if *Distance between MCS and current zone*$< \delta$ **then**
    $M = \{1, 2, ..., y+1\} \leftarrow M = \{1, 2, ..., y\}$
  end if
end for
1.2. Determine the final number of DEVs as f and the total number of charging services available as n.
2. **for** *each,* $j \in J$ **do**
  2.1 Calculate d_j^{th} using (3.1) then prioritize DEVs based on this value.
  2.2. Calculate $d_{k,l}$ and Dis as $d_{j,l}$, $d_{j,i}$, $d_{j,h}$, and $d_{j,m}$.
  2.3. Calculate q_j from (3.3).
end for
3. **for** *each,* $a \in L, I, H, M$ **do**
  if $Dis < d_j^{th}$ **then**
    Collect MPs, FCSs, HCSs, and MCSs locations as charging locations.
  end if
end for
4. **for** *each,* $j \in J$ **do**
  Using Dis in step 2.2, choose the charging locations among collected MPs, FCSs, HCSs, or MCSs locations with minimum distance.
end for
5. **if** n>=f **then**
  5.1. **for** *each,* $a \in L, I, H, M$ **do**
    Replace the selected charging locations for some DEVs with lower priority with other charging locations that satisfy step 3, so that an ideal number of DEVs is assigned to each available charging location.
  end for
  5.2. **for** *each,* $j \in J$ **do**
    if *DEV j is assigned to charge at assigned MP l with a SEV* **then**
      5.2.1. **for** *each,* $k \in K$ **do**
        Use $d_{j,l}$ and $d_{k,l}$ results from step 2.
        Initialize p_k, v_k, c_k^e
        Calculate $c_{j,l}^t$ from (3.4), c_j^{ti} from (3.5), $c_{j,l}$ from (3.2), c_k^b from (3.10), $c_{k,l}^t$ from (3.8), and t_j^w from (3.6).
      end for
      5.2.2. Create a matrix with elements filled with the calculated $c_{j,l}$.
      5.2.3. Use the Hungarian algorithm to find the best-matched DEVs and SEVs so that the cost is minimized.
    else
      5.2.4. Calculate c_j^{ti} for DEV, $c_{j,i}$ and $c_{j,h}$ from (3.11), $c_{j,m}$ from (3.13), c_k^b, and t_j^w.
      5.2.5. Consider FCSs, HCSs, and MCSs for charging the DEVs assigned to them.
    end if
    5.2.6. DEVs go towards allocated charging locations to get charged given their priorities.
  end for
else
  5.3. $Itr \leftarrow \lceil \frac{z}{n} \rceil$
  if $Itr <= 3$ **then**
    5.4. **for** *each,* $a \in I, H, M$ **do**
      Replace the selected charging locations for some DEVs with lower priority with other charging locations that satisfy step 3, ensuring the $Itr - 1$ number of DEVs is assigned to each FCS, HCS, and MCS location.
    end for
    5.5. From the DEVs not assigned to the FCSs, HCSs, and MCSs locations in the previous step, group an equal number with the number of SEVs that require a greater value of q_j to be matched with SEVs.
    5.6. **for** *selected* $l \in L$ **do**
      Replace the selected MPs for selected DEVs from the previous step with lower priority, ensuring one DEV is assigned to each MP.
    end for
    5.7. For grouped DEVs assigned to MPs during steps 5.5 and 5.6, and one DEV with higher priority assigned to each FCS, HCS, and MCS location in step 5.4, do step 5.2.
    5.8. Find unmatched DEVs
    5.9. **for** *each,* $k \in K$ **do**
      Calculate the new current SOC of SEVs.
    end for
    5.10. **if** $Itr == 2$ **then**
      5.10.1. Do steps 5.2.1 and 5.2.4 to calculate charging costs.
      5.10.2. Create a matrix with calculated charging costs.
      5.10.3. Use the Hungarian algorithm to assign unmatched DEVs with available SEVs and other available charging services.
      5.10.4. DEVs go toward allocated charging services to get charged.
    else
      5.10.5. **if** $Itr == 3$ **then**
        For unmatched DEVs, repeat step 5.2.
        Repeat steps 5.8., 5.9., and 5.10.1. to 5.10.4.
      end if
    end if
  else
    5.11. $Itr \leftarrow 3$
    5.12. Do steps 5.4. to 5.10.
  end if
end if

Output:
1. Calculate the total cost of charging DEVs as a summation of $c_{j,l}$, $c_{j,i}$, $c_{j,h}$, $c_{j,m}$ for all DEVs.
2. Calculate the total utility of sellers in all charging services as the summation of u_j^{ch} calculated using (3.15) for each charging service.
3. Calculate the total consuming time for all DEVs as the summation of consuming time defined as c_j^{ti}/α for DEV j.

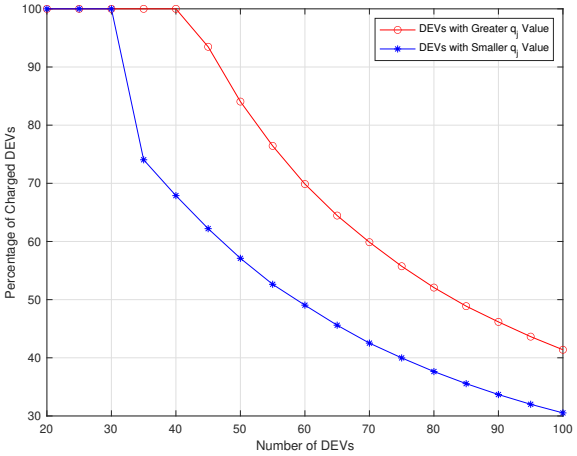

FIGURE 5.1: Comparison between grouping DEVs with greater q_j value and DEVs with smaller q_j value to achieve the maximum rate of charged DEVs in the state (c).

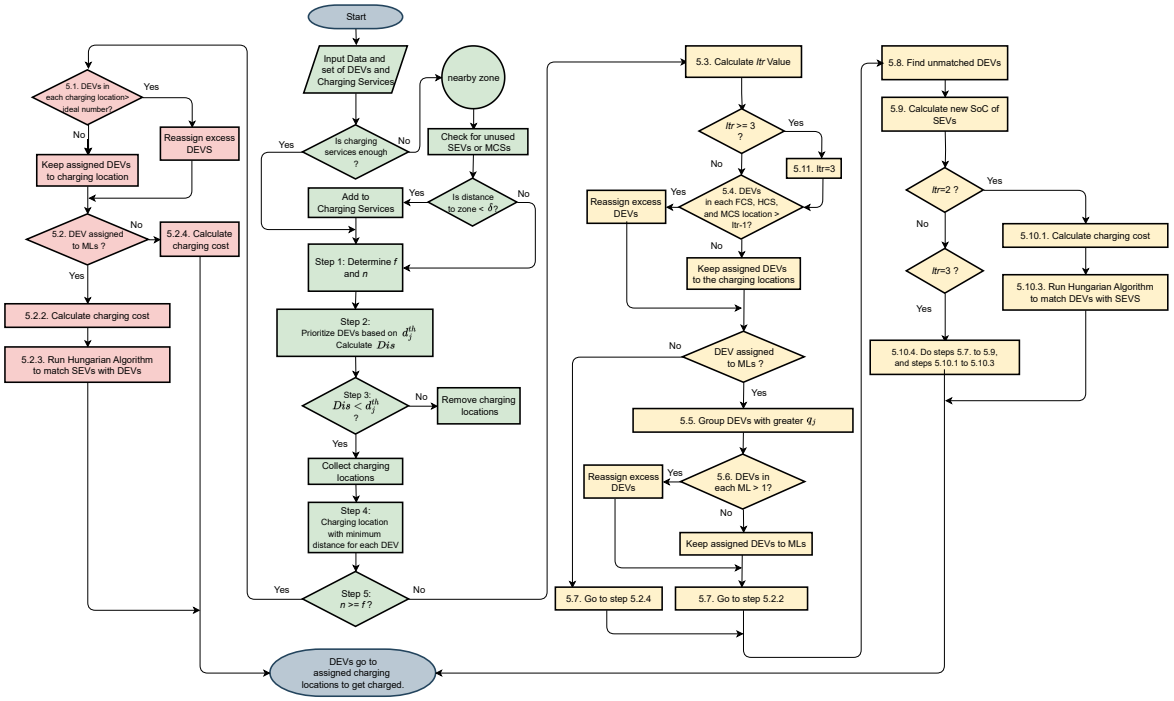

FIGURE 5.2: Flowchart of max capacity-based cooperative algorithm

were sourced from [85], as depicted in Figure 5.3. In this section, the simulations are conducted specifically for the first zone (the bottom one) defined within the boundaries of (0,0) and (20,10). This analysis considers a scenario where there are two FCSs in the zone and there might be insufficient charging services available. To address this issue, the fog node of the first zone utilizes SEVs and MCSs from the second zone to supplement the available charging services. Following this, the evaluation of states (a), (b), and (c) mentioned earlier takes place.

In the first state (a), where the DEVs number is less than the charging services number,

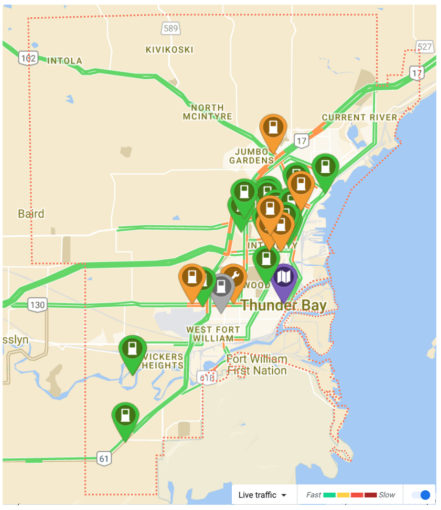

FIGURE 5.3: Deployment of FCSs in the Thunder Bay area, with traffic conditions represented by colors ranging from green indicating minimal traffic to maroon indicating the highest congestion.

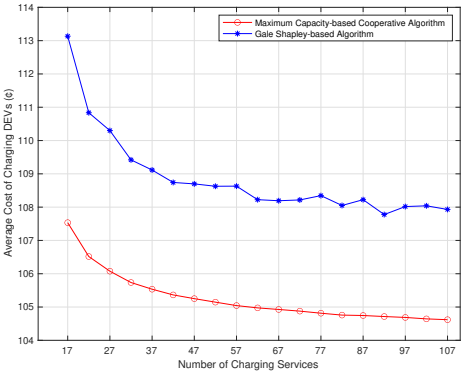

(a) DEVs number < charging services number

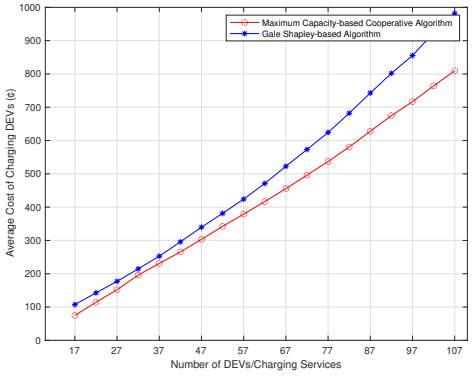

(b) DEVs number = charging services number

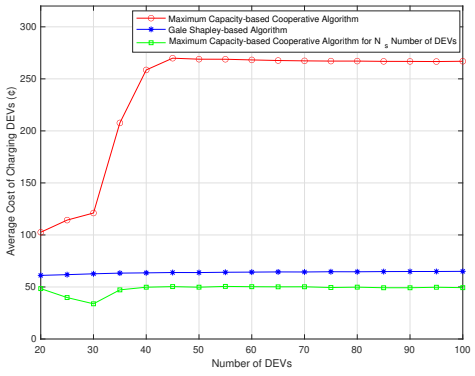

(c) DEVs number > charging services number

FIGURE 5.4: Average cost of charging DEVs with charging services for different three states.

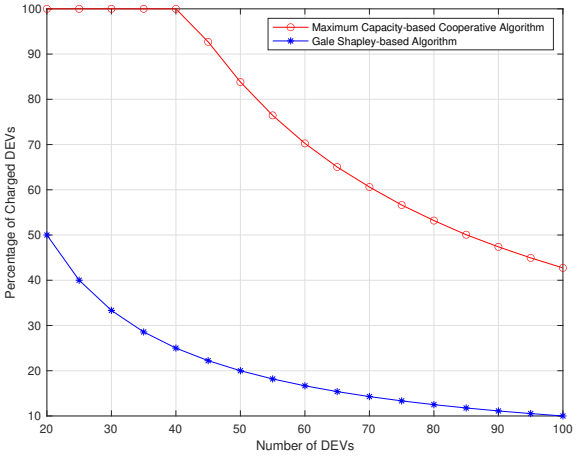

FIGURE 5.5: Percentage of charged DEVs in 3 cycles with 10 SEVs and DEVs varying from 20 to 100.

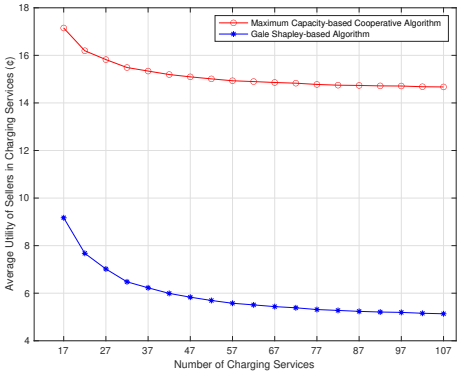

(a) DEVs number < charging services number

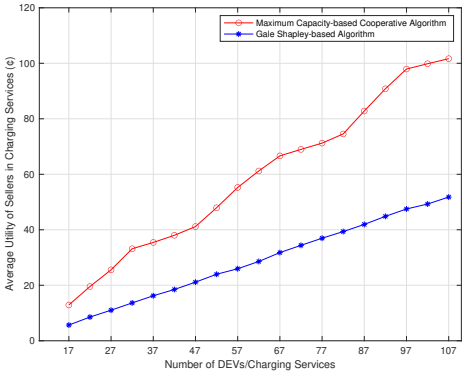

(b) DEVs number = charging services number

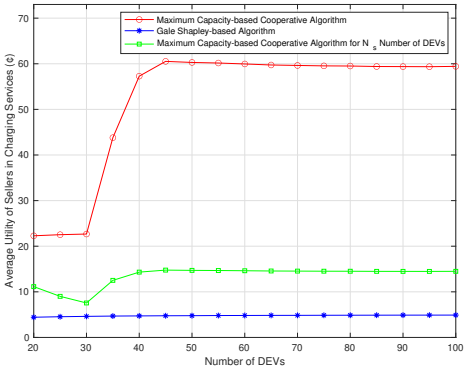

(c) DEVs number > charging services number

FIGURE 5.6: Comparison of average utility of sellers in charging services for three different states.

we assume that there are 10 DEVs and the number of SEVs can vary between 10 to 100, resulting in a range of charging services between 17 to 107. For this state, all

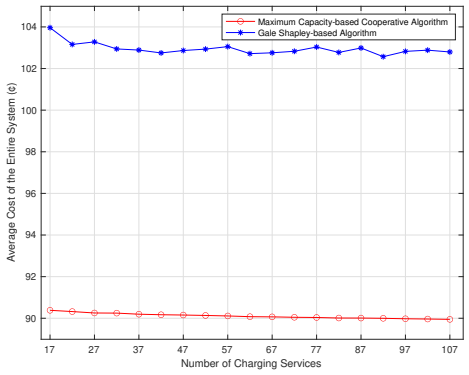

(a) DEVs number < charging services number

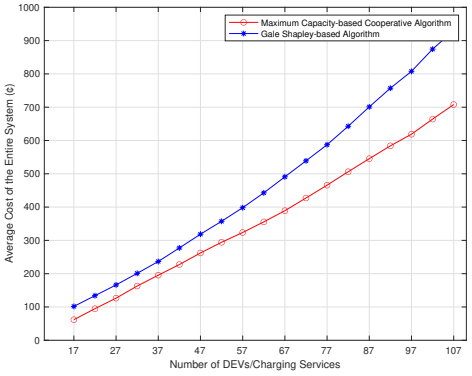

(b) DEVs number = charging services number

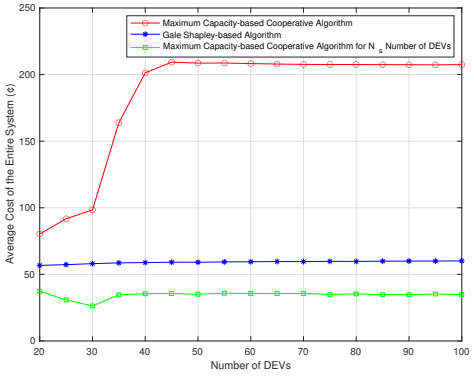

(c) DEVs number > charging services number

FIGURE 5.7: Comparison of average cost of the entire system for different states.

charging services are exclusively provided within the first zone, and their locations are limited to that zone. In the second state (b), the DEVs number is equal to the charging services number, the number of DEVs is a number between 17-107, and the number of SEVs between 10 to 100 results in the number of charging services between 17 to 107. When the number of DEVs exceeds the number of charging services (third state (c)), we assume the number of SEVs is equal to 10 resulting in 17 charging services, and the number of DEVs can be an amount between 20 to 100. In the case of (b) and (c) states, the first zone has some available SEVs but lacks any available MCSs. The fog node corresponding to this zone communicates with nearby fog nodes and uses two unused MCSs and some unused SEVs from the second zone, which is within a distance threshold of $\delta = 8$ km from the current zone. Consequently, the random SEV locations are distributed within the domain encompassing both the first zone and a portion of the second zone, covering the coordinate range from (0,0) to 20,18).

DEVs and SEVs following rectangular paths have their positions defined using a random function. Moreover, in our simulations, we employ the city block distance metric to

calculate distances between points. In our assumptions, two specific locations have been identified within the first zone at coordinates (6,9) and (16,9) which serve as "MCS locations" where two MCSs, from the first zone for the state (a) and from the second zone for states (b) and (c), come and remain stationary, awaiting the arrival of DEVs for the purpose of charging. Moreover, within the first zone, we take into account our dedicated charging services as two FCSs which are located in (10, 3) and (11, 8), and we assume that each FCS has two available spots for charging DEVs, and one HCS located in (15,6). Therefore, we have seven dedicated charging services and the number of SEVs as random charging services can be different in each state. The twenty-five MPs are distributed uniformly in the zone, with determined places at the beginning.

The following are the simulation parameters: p_0=14.8 Â¢/kWh [86], p_k=a uniform distribution of 20 to 30 Â¢/kWh, and α=7.25 \$/h [87]. r^e=40 kw, λ=95 %, c^r=150 \$/kwh, θ=0.27 %, soc_j^c=a uniform distribution of 10 to 20 %, soc_j^r=a uniform distribution of 50 to 80 % , soc_k^a=a uniform distribution of 80 to 90 % ,Γ=5 %, and v_j/v_k=A Gaussian distribution with a mean value of 60 km/h and a variance of 10 km/h (as typical city speed limits hover around 60 km/h), t_j^{idle}/t_k^{idle}=a uniform distribution of 0 to 5 min, $\delta = 8\,km$ The 250 common EV categories dataset from [88] is used for uniform selection of each EV type. The Battery Capacity b_j^c (kwh) and energy consumption rate c_j^e (kwh/km) of EVs are included in the dataset used for EV range prediction.

In order to assess the performance, we compare the Gale Shapley-based algorithm [3] with our proposed technique, the Maximum capacity-based cooperative algorithm. To ensure statistical significance, the results are averaged across 300 independent simulation runs.

5.2.2 Results and discussion

In this section, we examine the outcomes of Figures 5.4, 5.6, 5.7, 5.8, and 5.10 for all three aforementioned states. Additionally, we consider Figure 5.5 specifically for the state (c), and Figure 5.9 for the case where the number of DEVs is set to 10 and the number of SEVs is set to 10, resulting in a total of 17 charging services. In the case of Figures 5.4, 5.6, 5.7, and 5.8, states (a) and (b) consist of two curves, represented by red and blue lines, which compare the results obtained from our algorithm with those obtained from the Gale Shapley-based algorithm. In state (c), there are three curves depicted in different colors. The red line represents the total assessed value obtained from our algorithm, while the blue line represents the total assessed value when using the Gale Shapley-based algorithm. Additionally, we introduce a green curve in this figure to demonstrate the summation of the equal number of assessed values from both

our algorithm and the Gale Shapley-based algorithm, facilitating a comparison of the results. The following section describes the performance measurements used for assessing our algorithm. We adopt some of the performance measurements described in [3] and [15] are followed here.

5.2.3 Performance measurements

The performance measurements of our algorithm are as follows:

- $\overline{c}$ as average cost of charging DEVs: This average cost is defined by dividing the total charging costs of DEVs by the total amount of energy supplied for the minimum number of DEVs in each state [3]:

$$\overline{c} = \frac{\sum(c_{j,l} + c_{j,i} + c_{j,h} + c_{j,m})}{\sum(q_j)} \tag{5.1}$$

- $\overline{u}$ as the average utility of sellers in charging services: The average utility is defined as the sum of the acquired utility for all charging services, divided by the total amount of energy provided for the minimum number of DEVs in each state as:

$$\overline{u} = \frac{\sum(u_j^{ch})}{\sum(q_j)} \tag{5.2}$$

- $\overline{t}$ as average consuming time: This time is defined as the total time taken for all DEVs from the moment a DEV goes toward the designated charging service until the charging process is completed over the maximum time among the minimum number of DEVs in each state as:

$$\overline{t} = \frac{\sum(c_j^{ti}/\alpha)}{max(c_j^{ti}/\alpha)} \tag{5.3}$$

The subsequent sections present an evaluation of performance measurements for our algorithm. In the evaluation phase comparing our algorithm with the Gale-Shapley algorithm, we analyze the improvement percentage achieved by our algorithm over the Gale-Shapley algorithm across various performance metrics. This improvement is calculated using the following equation:

$$\text{improvement\_percentage} = \frac{\text{performance\_2} - \text{performance\_1}}{\text{performance\_1}} \times 100 \tag{5.4}$$

where 'Performance_1' denotes the performance measurement of the Gale-Shapley algorithm, while 'Performance_2' represents the performance measurement of our proposed algorithm.

For Figures 5.4, 5.6, 5.7, and 5.8 across all three states, we calculate the mean value of these improvement percentage as follows:

$$\text{mean\_improvement\_percentage} = \frac{(\sum \text{improvement\_percentage})}{\text{num}} \tag{5.5}$$

For state (a), where the number of charging services varies between 17 to 107, num = 19. Therefore, to compute the mean value of the improvement percentage in this state, we calculate the improvement percentage using (5.4) for each value of charging service number and then find the summation of these values over 19, representing the different values for the number of charging services in state (a). In state (b), where the number of DEVs and charging services ranges from 17 to 107, we set num = 19. We follow a similar approach by computing the improvement percentage using (5.4) for each value of DEVs or charging service number. Then, we sum up these values over 19, which represents the varying values for DEVs/charging services number in state (b). For state (c), where the number of DEVs ranges from 20 to 100, num = 17. Hence, to determine the mean value of the improvement percentage in this state, we calculate the improvement percentage using (5.4) for each value of DEVs number, and then find the summation of these values over 17, representing the different values for DEVs number in state (c).

In Figure 5.9, we assess the impact of changing the provider energy price, value of time, and upper limit for idling time spent in traffic on the average cost of charging DEVs. Specifically, in Figure 5.9-a, we observe the gradual increase of energy price from 20 to 30. In Figure 5.9-b, we analyze the progressive rise in the value of time from 7 to 20. Lastly, in Figure 5.9-c, we examine the incremental increase in the upper limit for idling time spent in traffic. When calculating the mean value of the improvement percentage in 5.5, for Figure 5.9-a, we set num = 11 to account for the different values for the energy price parameter. For Figure 5.9-b, num = 14 is chosen to represent the various values for the value of time parameter. Finally, for Figure 5.9-c, where the upper limit rises incrementally from 1 to 20, num = 20 is utilized to encompass the different values for the upper limit for idling time spent in traffic parameter.

5.2.4 Average cost of charging DEVs

In figure 5.4, the average cost of charging DEVs, $\bar{c}$, is shown. The comparison is made between the proposed Maximum capacity-based cooperative algorithm and the Gale-Shapley algorithm for states (a),(b), and (c). As can be seen in Figure 5.4-a, the average cost of charging DEVs for our algorithm is less than the Gale Shapley-based one. The improvement percentage for the average cost of charging DEVs in this state, for each value of charging services number, is derived from 5.4. We then compute the mean value of this improvement percentage across all values for the number of charging services using 5.5. The resulting value is -3.3088, signifying an average decrease of 3.3088% in the average cost of DEVs across all numbers of charging services. Furthermore, it is notable that the more the number of charging services the less the total cost. This is due to the fact that a higher number of charging services gives a better opportunity to DEVs to find the service with less charging cost.

The total cost again is minimized for state (b) as seen in Figure 5.4-b. The mean value of improvement percentage regarding the average charging cost for DEVs in state (b) stands at -14.3370, signifying a reduction in the average cost by 14.3370% across all values for DEVs/charging services number. In addition, it indicates the summation of the charging cost for DEVs increases as the number of DEVs/charging services increases.

In figure 5.4-c, the red line shows the total cost of charging DEVs resulting from using the proposed algorithm. Since our algorithm benefits from one-to-multiple charging of more than 10 vehicles, it is reasonable that the curve tends to be ascending when increasing the number of DEVs. The blue graph shows the cost of charging when using the Gale Shapley-based algorithm as a one-to-one method which gives rise to charging of only 10 DEVs. The green curve depicts the total cost of charging 10 DEVs compared to the Gale Shapley-based method using the same criteria showing that this profile sits beneath the blue one. For state (c), the mean value of improvement percentage is -24.8117 showing a decrease of 24.8117% in the average cost.

5.2.5 Percentage of charged DEVs

Figure 5.5 shows the percentage of DEVs that can be charged in 3 cycles of sending DEVs to charging services. For this simulation, the number of SEVs=10 results in the number of charging services=17, and the number of DEVs varies from 20 to 100. As can be seen, the Gale Shapley-based algorithm can only charge 10 DEVs which was expected as a one-to-one matching method. Our algorithm, however, allows for %100 charge of DEVs as long the number of DEVs does not exceed 40. After this

point when more DEVs are joined, the charging algorithm, would not be able to meet the demand, leading to decreasing in the percentage of charged DEVs as the number of DEVs increases. However, this ratio shows to be dropping more gently than that of the Gale Shapley-based algorithm. Figures 5.4-c and 5.5 clearly demonstrate that implementing the Maximum Capacity-based cooperative algorithm leads to a reduction in cost and an increase in the number of charged DEVs.

5.2.6 Average utility of sellers in charging services

Figure 5.6 shows the average utility of sellers in charging services, $\overline{u}$. This performance measurement is evaluated for both the Gale Shapley-based algorithm and the Maximum Capacity-based cooperative algorithm across the three states mentioned earlier. The simulation results show that charging services can trade energy with a positive utility value, which provides an incentive for SEVs as dynamic random charging services with excess energy to contribute to the V2V charging process. In each state, our proposed algorithm offers a larger utility for the charging services compared to the Gale Shapley-based method.

Observing Figure 5.6-a, it is noticeable that the utility tends to decrease with a larger number of charging services because, in this case, there are more alternatives for suppliers, and the DEVs are more likely to choose those with lower offering costs. Figure 5.6-b also shows the as-expected results of increasing the total utility value as the number of DEVs/charging services rises. In Figure 5.6-c, the green curve associated with charging services used for charging 10 DEVs shows to outperform the Gale Shapley-based curve in terms of the amount of utility.

In terms of average utility, the mean improvement percentages, as obtained from 5.5, are 160.3684, 109.2073, and 182.0265 for states (a), (b), and (c) respectively. It indicates an increase in the average utility of sellers across all three states. The apparent disparity in the percentage improvement for utility compared to that of cost stems from the fact that the initial utility value is considerably smaller than the initial cost value. Consequently, the same absolute change has a proportionally larger impact on the smaller initial value, resulting in a seemingly higher percentage improvement for utility.

5.2.7 Average cost of the entire system

The average cost of the entire system is presented in Figure 5.7. This value is obtained by subtracting the average utility of sellers in charging services (Figure 5.6) from the average cost of charging DEVs (Figure 5.4) as $\overline{c} - \overline{u}$. The cost of the entire system will be

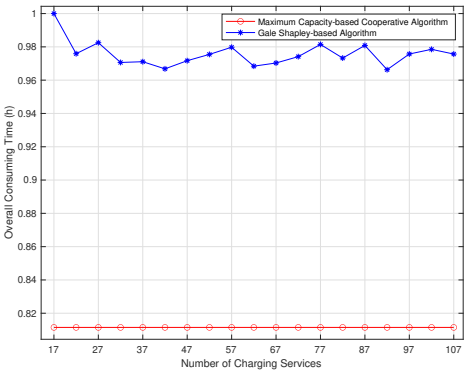

(a) DEVs number < charging services number

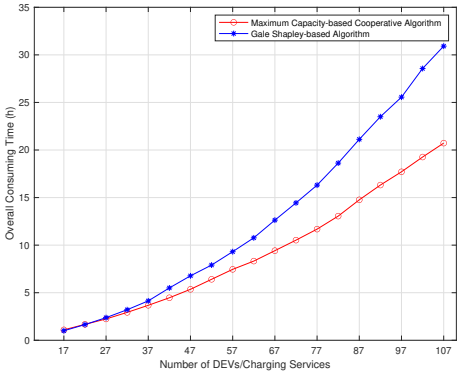

(b) DEVs number = charging services number

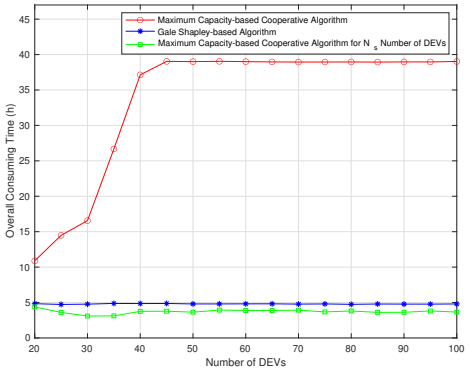

(c) DEVs number > charging services number

FIGURE 5.8: Comparison of average consuming time of DEVs for three different states.

lower for the Maximum capacity-based cooperative algorithm than for the Gale-Shapley algorithm for all three states. The mean improvement percentages for our algorithm over the Gale-Shapley algorithm, obtained from 5.5, are -12.4685, -22.1068, and -41.5239 for states (a), (b), and (c) respectively. This signifies a decrease of 12.4685%, 22.1068%, and 41.5239% in the average cost of the entire system across all three states.

5.2.8 Average consuming time of DEVs

Figure 5.8 shows the average consuming time, $\bar{t}$, of DEVs for both algorithms. The average consuming time for the Maximum capacity-based cooperative algorithm is lower than the Gale-Shapley approach. The mean value of percentage of improvement, obtained from 5.5, for state (a) is -16.8259, for state (b) is -20.1818, and for state (c) is -22.6292. It shows a decrease of 16.8259%, 20.1818%, and 22.6292% in the average consuming time for three states. It is because, for the Maximum capacity-based cooperative algorithm, the EV user's time is taken into account during the optimization procedure with the purpose of limiting and optimizing it. Indeed, our algorithm takes cost, time,

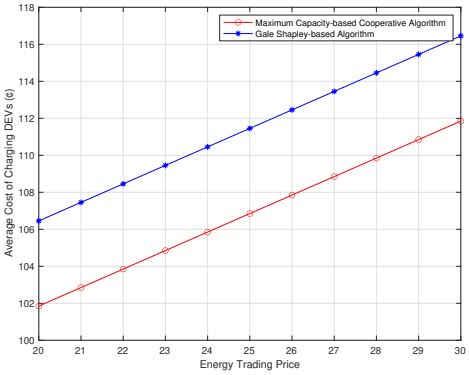

(a) Changing provider energy unit price

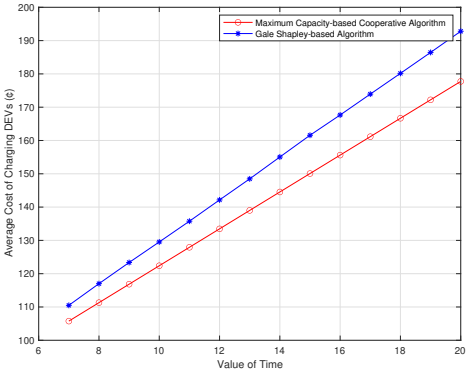

(b) Changing Value of Time

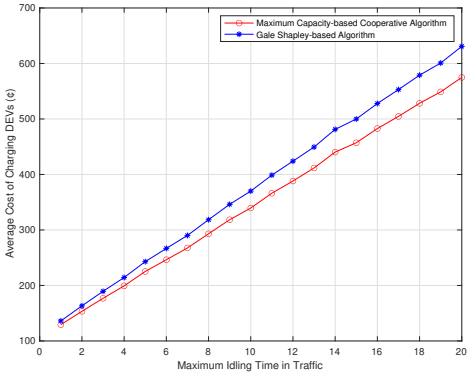

(c) Upper Limit for Idling Time Spent in Traffic

FIGURE 5.9: Impact of changing above parameters on average cost of charging DEVs when DEVs and SEVs number = 10.

and minimizing the DEVs with range anxiety into account during charging locations selection and final matching. On the other hand, compared to the Gale Shapley-based method, as mentioned before, our algorithm reduces this time regarding the availability of charging services stemming from using the maximum capacity of each of them in the time of being assigned to DEVs.

5.2.9 Impact of time valuation, energy trading price, and the upper limit for idling time spent in traffic

In this subsection, we evaluate the impact of changing three parameters in the average cost of DEVs. In this experiment, the number of DEVs and SEVs is held constant at 10 each, resulting in a total of 17 charging services for each operation. The impact of changing the energy price is examined in Figure 5.9-a, where the average cost of charging DEVs is analyzed as the energy price gradually increases from 20 to 30. The

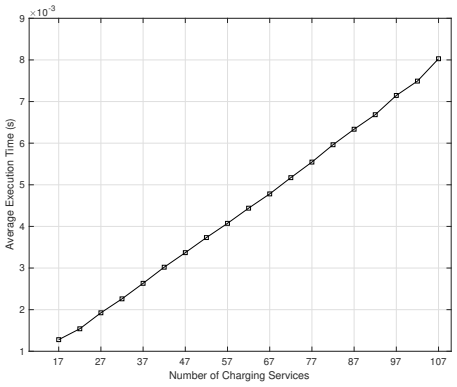

(a) DEVs number < charging services number

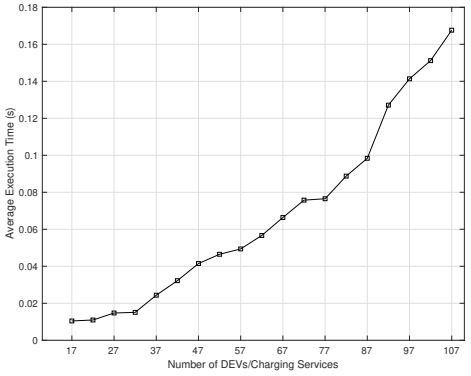

(b) DEVs number = charging services number

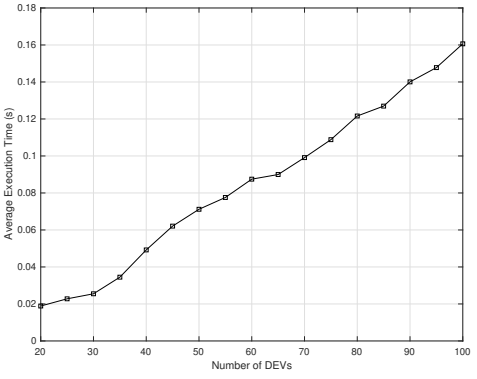

(c) DEVs number > charging services number

FIGURE 5.10: Average execution time of Maximum capacity-based cooperative algorithm for three different states.

mean improvement percentage for the average cost of charging DEVs resulting from this energy price change is −4.1348, indicating a 4.1348% decrease in the average cost.

Similarly, the effect of changing the value of time is depicted in Figure 5.9-b. Here, the average cost of charging DEVs is evaluated as the value of time progressively rises from 7 to 20. The mean improvement percentage for the average cost of charging DEVs resulting from this change in the value of time is −6.3986, demonstrating a 6.3986% decrease in the average cost.

Furthermore, Figure 5.9-c illustrates the impact of increasing the upper limit for idling time spent in traffic on the average cost of charging DEVs. As the upper limit incrementally rises from 1 to 20, the cost of charging for our algorithm consistently remains lower than that of the Gale Shapley-based approach. The mean improvement percentage for the average cost of charging DEVs resulting from this change in the upper limit for idling time spent in traffic is −7.8581, indicating a 7.8581% decrease in average cost.

5.2.10 Execution time

Figure 5.10 depicts the average execution time of the algorithm. For each run, and for each state, we run the algorithm 3000 times. As can be seen from figure 5.10, the time execution follows a linear behavior.

5.3 Summary

This chapter introduces a maximum capacity-based cooperative algorithm designed to facilitate energy trading between DEVs and available charging services in a collaborative manner. The primary objective is to minimize the charging cost of DEVs, decrease waiting times, and boost the rate of charged DEVs. Practical scenarios for varying numbers of DEVs and charging services are implemented. Evaluation of numerical results demonstrates that our algorithm outperforms the Gale-Shapley based algorithm in performance measurements, including the average cost of charging DEVs, the average utility of sellers in charging services, the average consumption time, and the percentage of charged DEVs.

Chapter 6

Conclusions and Future Work

6.1 Conclusions

we proposed a cooperative charging strategy in this work, using the Hungarian matching method, allowing EV drivers who are anxious about range anxiety to acquire energy from other EVs with a excess charge, FCSs, HCSs, and MCSs. To improve energy exchanges, the system is divided into zones, and the trading strategy within every zone is optimized. Our solution was numerically evaluated by comparing it to the Gale Shapley-based charging mechanism. According to the numerical results, our algorithm can keep costs and consuming time down while simultaneously enhancing the rate of charged EVs by taking into account one-to-multiple matched EVs and optimal collaboration between SEVs and other charging services for charging DEVs. we proposed cooperative fashion energy exchanges to prevent overloads of distribution transformers caused by massive EV charging demands occurring at the same time. This approach consequently allows the exchange of energy between EVs and charging services while also controlling EVs more actively, in a more cost-effective manner.

Furtheremore, as a part of our proposed matching algorithm, in the initial steps, we prioritized DEVs based on the maximum distance they can go with their current SoC.This prioritization benefits EV users with lower remaining ranges, alleviating their range anxiety and addressing their charging concerns. Precise estimation of EV driving range is crucial for mitigating driver anxiety during trips and improving overall trip planning convenience. Consequently, in this work, we developed a robust predictive model for estimating EV driving range, integral to promoting DEVs in our matching algorithm. Leveraging large samples of real driving data collected from authentic sources, the proposed models are evaluated. The extensive ablation study reveals that the proposed

ensemble model exploiting the strength of MLR and XGBoost techniques stands out as the most effective approach.

6.2 Future Work

In this section, we propose several ideas for extending and improving upon the current work. These ideas aim to extend various aspects of the system model and algorithms, potentially enhancing their practicality and effectiveness in real-world scenarios.

- **Enhanced Communication Protocol Analysis:** In the system model described in Chapter 3, we employed DSRC communication protocols for facilitating communication between RSUs acting as fog nodes and EVs and charging services as IoT devices. As a future endeavor, we could delve deeper into analyzing the performance of these communication protocols. This analysis could involve calculating key performance metrics such as Signal-to-Noise Ratio (SNR), throughput, latency, and reliability. Comparing these metrics with those obtained from alternative protocols could provide valuable insights into the effectiveness and efficiency of the chosen communication approach.

- **Augmented Energy Trading:** Our system model introduced a matching algorithm for energy trading, focusing on critical factors such as the cost of DEVs, the utility of sellers in charging services, consuming time, and the rate of charged DEVs. As a potential enhancement, we could extend the algorithm to incorporate additional considerations, such as user privacy and data security during the payment process. Integrating these aspects could further enhance the robustness and applicability of the energy trading system.

- **Dynamic Energy Price Modeling:** While our proposed algorithm in Chapter 5 assumes a predefined energy price, in practice, this price may vary based on various factors. To address this, we could explore the integration of dynamic pricing models within the matching algorithm. This could involve incorporating factors such as scheduling and timing into the pricing formula outlined in Chapter 3. Additionally, developing ML models to predict energy prices based on influencing factors could enable a more adaptive and practical matching process.

- **Algorithmic Diversification:** Our proposed matching algorithm in Chapter 5 utilizes the Hungarian matching algorithm as a key component. As a future investigation, we could explore alternative matching algorithms and assess their performance within the context of our system model. Comparing the outcomes obtained

with different algorithms could offer insights into their comparative strengths and weaknesses, potentially guiding algorithmic selection for specific deployment scenarios.

- **Predictive System Modeling:** In our system model, we rely on predefined values for parameters such as energy consumption, EV speeds, and traffic congestion levels. To enhance the realism of the model, we could develop predictive models using ML techniques. These models could analyze influencing factors to predict the aforementioned parameters accurately. By integrating predictive modeling, we could achieve a more dynamic and adaptable system model, better aligned with real-world conditions.

Appendix A

Results of Ten-Fold CV and Final Predictive Model Implementation using PCA Technique

The tables presented below display the outcomes obtained from utilizing the PCA technique with ten principal components for feature engineering during the development of our ML models in Chapter 4. A comparison with the results obtained from the CA technique, as depicted in Tables 4.2 and 4.4, representing the CA technique for ten-fold CV and Final Predictive Model Implementation using the CA Technique respectively. It indicates that the results of CA analysis outperform those of PCA analysis in both ten-fold CV and the final implementation of ML models.

Table A.1: Ten-Fold CV results of various ML models considered in this study Using PCA technique

Model	Average MAE	Best MAE	Average R2	Best R2
ELM	25.84	25.271	0.7	0.719
XGBoost	22.184	21.424	0.776	0.804
MLR	32.756	32.183	0.573	0.592
MLP	24.21	23.771	0.743	0.766
Deep MLP	17.829	16.552	0.816	0.845
RF	17.306	16.677	0.83	0.858
AdaBoost	26.592	25.946	0.714	0.739
SVR	27.938	27.338	0.512	0.532

TABLE A.2: Quantitative analysis of the final models built using single training and hold-out sets and their performances using PCA technique.

Model	Training MAE	Test MAE	Training R2	Test R2	Inference Time (s)
ELM	25.032	26.078	0.695	0.706	40.2894
XGBoost	20.638	21.252	0.813	0.79	4.32321
MLR	32.753	42.636	0.577	0.436	4.41784
MLP	23.426	52.648	0.762	0.236	66.8106
Deep MLP	17.517	50.748	0.83	0.497	29.2298
RF	13.951	17.201	0.896	0.815	13.0786
AdaBoost	25.11	25.979	0.756	0.692	10.5717
RF and XGBoost	13.71	16.847	0.901	0.826	45.5463
MLR and XGBoost	20.107	21.802	0.817	0.772	6.08268
RF and MLP	13.778	17.144	0.897	0.836	364.264

References

[1] Chen Chen, Lanlan Chen, Lei Liu, Shunfan He, Xiaoming Yuan, Dapeng Lan, and Zhuang Chen. Delay-optimized v2v-based computation offloading in urban vehicular edge computing and networks. *IEEE Access*, 8:18863–18873, 2020.

[2] Alexandros-Michail Koufakis, Emmanouil S Rigas, Nick Bassiliades, and Sarvapali D Ramchurn. Offline and online electric vehicle charging scheduling with v2v energy transfer. *IEEE Transactions on Intelligent Transportation Systems*, 21(5):2128–2138, 2019.

[3] Mohammed Shurrab, Shakti Singh, Hadi Otrok, Rabeb Missouri, Vinod Khadkikar, and Hatem Zeineldin. A stable matching game for v2v energy sharing-a user satisfaction framework. *IEEE Transactions on Intelligent Transportation Systems*, 2021.

[4] Jie Zhang, Qiang Tang, Shuohan Liu, Yue Cao, Wei Zhao, Tao Liu, and Shiming Xie. Deadline-based v2v charging under spatial resource constraints. In *2021 International Conference on Control, Automation and Information Sciences (ICCAIS)*, pages 240–245. IEEE, 2021.

[5] Yue Cao, Tao Jiang, Omprakash Kaiwartya, Hongjian Sun, Huan Zhou, and Ran Wang. Toward pre-empted ev charging recommendation through v2v-based reservation system. *IEEE transactions on systems, man, and cybernetics: systems*, 51(5):3026–3039, 2019.

[6] Long Zeng, Canbing Li, Zuyi Li, Mohammad Shahidehpour, Bin Zhou, and Quan Zhou. Hierarchical bipartite graph matching method for transactive v2v power exchange in distribution power system. *IEEE Transactions on Smart Grid*, 12(1):301–311, 2020.

[7] Eyuphan Bulut and Mithat C Kisacikoglu. Mitigating range anxiety via vehicle-to-vehicle social charging system. In *2017 IEEE 85th Vehicular Technology Conference (VTC Spring)*, pages 1–5. IEEE, 2017.

[8] Miao Wang, Muhammad Ismail, Ran Zhang, Xuemin Shen, Erchin Serpedin, and Khalid Qaraqe. Spatio-temporal coordinated v2v energy swapping strategy for mobile pevs. *IEEE Transactions on Smart Grid*, 9(3):1566–1579, 2016.

[9] Xiaolin Mou, Rui Zhao, and Daniel T Gladwin. Vehicle-to-vehicle charging system fundamental and design comparison. In *2019 IEEE International Conference on Industrial Technology (ICIT)*, pages 1628–1633. IEEE, 2019.

[10] Mohammad Ekramul Kabir, Ibrahim Sorkhoh, Bassam Moussa, and Chadi Assi. Joint routing and scheduling of mobile charging infrastructure for v2v energy transfer. *IEEE Transactions on Intelligent Vehicles*, 6(4):736–746, 2021.

[11] Guangyu Li, Qiang Sun, Lila Boukhatem, Jinsong Wu, and Jian Yang. Intelligent vehicle-to-vehicle charging navigation for mobile electric vehicles via vanet-based communication. *IEEE Access*, 7:170888–170906, 2019.

[12] Mohammed Shurrab, Shakti Singh, Hadi Otrok, Rabeb Mizouni, Vinod Khadkikar, and Hatem Zeineldin. An efficient vehicle-to-vehicle (v2v) energy sharing framework. *IEEE Internet of Things Journal*, 9(7):5315–5328, 2021.

[13] Guangyu Li, Chen Gong, Lin Zhao, Jinsong Wu, and Lila Boukhatem. An efficient reinforcement learning based charging data delivery scheme in vanet-enhanced smart grid. In *2020 IEEE International conference on big data and smart computing (BigComp)*, pages 263–270. IEEE, 2020.

[14] K Aravindhan, SKB Sangeetha, K Periyakaruppan, E Manoj, R Sivani, and S Ajithkumar. Smart charging navigation for vanet based electric vehicles. In *2021 7th International Conference on Advanced Computing and Communication Systems (ICACCS)*, volume 1, pages 1588–1591. IEEE, 2021.

[15] Rongqing Zhang, Xiang Cheng, and Liuqing Yang. Flexible energy management protocol for cooperative ev-to-ev charging. *IEEE Transactions on Intelligent Transportation Systems*, 20(1):172–184, 2018.

[16] Shahid A Hasib, Dip K Saha, S Islam, Mahib Tanvir, and Md Shahinur Alam. Driving range prediction of electric vehicles: A machine learning approach. In *2021 5th International Conference on Electrical Engineering and Information Communication Technology (ICEEICT)*, pages 1–6. IEEE, 2021.

[17] Xinyi Ye, Yanqi Zhang, Yiyang Ni, Qin Wang, and Yan Chen. Motivational game-theoretic vehicle-to-vehicle energy trading in the smart grid. In *2020 IEEE/CIC International Conference on Communications in China (ICCC Workshops)*, pages 231–236. IEEE, 2020.

[18] Muhammad Ikram Ashraf, Mehdi Bennis, Cristina Perfecto, and Walid Saad. Dynamic proximity-aware resource allocation in vehicle-to-vehicle (v2v) communications. In *2016 IEEE Globecom Workshops (GC Wkshps)*, pages 1–6. IEEE, 2016.

[19] Kan Zheng, Fei Liu, Qiang Zheng, Wei Xiang, and Wenbo Wang. A graph-based cooperative scheduling scheme for vehicular networks. *IEEE transactions on vehicular technology*, 62(4):1450–1458, 2013.

[20] Muhammad Ikram Ashraf, Chen-Feng Liu, Mehdi Bennis, Walid Saad, and Choong Seon Hong. Dynamic resource allocation for optimized latency and reliability in vehicular networks. *IEEE Access*, 6:63843–63858, 2018.

[21] Eyuphan Bulut, Mithat C Kisacikoglu, and Kemal Akkaya. Spatio-temporal non-intrusive direct v2v charge sharing coordination. *IEEE Transactions on Vehicular Technology*, 68(10):9385–9398, 2019.

[22] Elarbi Badidi, Zineb Mahrez, and Essaid Sabir. Fog computing for smart citiesâ big data management and analytics: A review. *Future Internet*, 12(11):190, 2020.

[23] Maanak Gupta, James Benson, Farhan Patwa, and Ravi Sandhu. Secure v2v and v2i communication in intelligent transportation using cloudlets. *IEEE Transactions on Services Computing*, 15(4):1912–1925, 2020.

[24] Liang Zhao, Wei Yao, Yu Wang, and Jie Hu. Machine learning-based method for remaining range prediction of electric vehicles. *IEEE Access*, 8:212423–212441, 2020.

[25] Bohan Zheng, Peter He, Lian Zhao, and Hongwei Li. A hybrid machine learning model for range estimation of electric vehicles. In *2016 IEEE Global Communications Conference (GLOBECOM)*, pages 1–6. IEEE, 2016.

[26] Irfan Ullah, Kai Liu, Toshiyuki Yamamoto, Rabia Emhamed Al Mamlook, and Arshad Jamal. A comparative performance of machine learning algorithm to predict electric vehicles energy consumption: A path towards sustainability. *Energy & Environment*, 33(8):1583–1612, 2022.

[27] Shuai Sun, Jun Zhang, Jun Bi, Yongxing Wang, et al. A machine learning method for predicting driving range of battery electric vehicles. *Journal of Advanced Transportation*, 2019, 2019.

[28] Cedric De Cauwer, Wouter Verbeke, Thierry Coosemans, Saphir Faid, and Joeri Van Mierlo. A data-driven method for energy consumption prediction and energy-efficient routing of electric vehicles in real-world conditions. *Energies*, 10(5):608, 2017.

[29] Changjong Kim, Yongseok Son, and Sunggon Kim. Towards access pattern prediction for big data applications. In *2022 13th International Conference on Information and Communication Technology Convergence (ICTC)*, pages 1577–1580. IEEE, 2022.

[30] Luiz Fernando Silva Pinto and Carlos Denner dos Santos. Motivations of crowdsourcing contributors. *Innovation & Management Review*, 15(1):58–72, 2018.

[31] Yuxiang Chris Zhao and Qinghua Zhu. Effects of extrinsic and intrinsic motivation on participation in crowdsourcing contest: A perspective of self-determination theory. *Online Information Review*, 38(7):896–917, 2014.

[32] Alexandros-Michail Koufakis, Emmanouil S Rigas, Nick Bassiliades, and Sarvapali D Ramchurn. Towards an optimal ev charging scheduling scheme with v2g and v2v energy transfer. In *2016 IEEE International Conference on Smart Grid Communications (SmartGridComm)*, pages 302–307. IEEE, 2016.

[33] Guangyu Li, Lila Boukhatem, Lin Zhao, and Jinsong Wu. Direct vehicle-to-vehicle charging strategy in vehicular ad-hoc networks. In *2018 9th IFIP International Conference on New Technologies, Mobility and Security (NTMS)*, pages 1–5. IEEE, 2018.

[34] Roberto Alvaro-Hermana, Jesus Fraile-Ardanuy, Pedro J Zufiria, Luk Knapen, and Davy Janssens. Peer to peer energy trading with electric vehicles. *IEEE Intelligent Transportation Systems Magazine*, 8(3):33–44, 2016.

[35] Rongqing Zhang, Xiang Cheng, and Liuqing Yang. Stable matching based cooperative v2v charging mechanism for electric vehicles. In *2017 IEEE 86th Vehicular Technology Conference (VTC-Fall)*, pages 1–5. IEEE, 2017.

[36] Fatih Yucel, Kemal Akkaya, and Eyuphan Bulut. Efficient and privacy preserving supplier matching for electric vehicle charging. *Ad Hoc Networks*, 90:101730, 2019.

[37] Jiawen Kang, Rong Yu, Xumin Huang, Sabita Maharjan, Yan Zhang, and Ekram Hossain. Enabling localized peer-to-peer electricity trading among plug-in hybrid electric vehicles using consortium blockchains. *IEEE Transactions on Industrial Informatics*, 13(6):3154–3164, 2017.

[38] Fatih Yucel, Eyuphan Bulut, and Kemal Akkaya. Privacy preserving distributed stable matching of electric vehicles and charge suppliers. In *2018 IEEE 88th Vehicular Technology Conference (VTC-Fall)*, pages 1–6. IEEE, 2018.

[39] Murat Yilmaz and Philip T Krein. Review of battery charger topologies, charging power levels, and infrastructure for plug-in electric and hybrid vehicles. *IEEE transactions on Power Electronics*, 28(5):2151–2169, 2012.

[40] Salman Habib, Muhammad Mansoor Khan, Farukh Abbas, and Houjun Tang. Assessment of electric vehicles concerning impacts, charging infrastructure with unidirectional and bidirectional chargers, and power flow comparisons. *International Journal of Energy Research*, 42(11):3416–3441, 2018.

[41] Riddhee Abhyankar, Ritesh Kumar Keshri, Pallavi Mahure, and Giuseppe Buja. Sizing and operation of a wireless power transfer system for bidirectional v2v energy exchange. In *IECON 2020 The 46th Annual Conference of the IEEE Industrial Electronics Society*, pages 2075–2080. IEEE, 2020.

[42] Utkarsha Sheshrao Bulkunde, Ritesh Kumar Keshri, Giuseppe Buja, and HM Suryawanshi. Phase shift control for v2v contactless energy exchange. In *2021 IEEE Transportation Electrification Conference (ITEC-India)*, pages 1–6. IEEE, 2021.

[43] Xiaolin Mou, Rui Zhao, and Daniel T Gladwin. Vehicle to vehicle charging (v2v) bases on wireless power transfer technology. In *IECON 2018-44th Annual Conference of the IEEE Industrial Electronics Society*, pages 4862–4867. IEEE, 2018.

[44] Xiaolin Mou, Daniel T Gladwin, Rui Zhao, Hongjian Sun, and Zhile Yang. Coil design for wireless vehicle-to-vehicle charging systems. *IEEE Access*, 8:172723–172733, 2020.

[45] Pengcheng You and Zaiyue Yang. Efficient optimal scheduling of charging station with multiple electric vehicles via v2v. In *2014 IEEE International Conference on Smart Grid Communications (SmartGridComm)*, pages 716–721. IEEE, 2014.

[46] Seyedfoad Taghizadeh, M Jahangir Hossain, Noushin Poursafar, Junwei Lu, and Georgios Konstantinou. A multifunctional single-phase ev on-board charger with a new v2v charging assistance capability. *IEEE Access*, 8:116812–116823, 2020.

[47] Tiago JC Sousa, Vítor Monteiro, JC Aparício Fernandes, Carlos Couto, Andrés A Nozueiras Meléndez, and João L Afonso. New perspectives for vehicle-to-vehicle (v2v) power transfer. In *IECON 2018-44th Annual Conference of the IEEE Industrial Electronics Society*, pages 5183–5188. IEEE, 2018.

[48] Sai Krishna Vempalli, K Deepa, et al. A novel v2v charging method addressing the last mile connectivity. In *2018 IEEE International Conference on Power Electronics, Drives and Energy Systems (PEDES)*, pages 1–6. IEEE, 2018.

[49]

[50] Mohd Rizwan Khalid, Irfan A Khan, Salman Hameed, M Syed Jamil Asghar, and Jong-Suk Ro. A comprehensive review on structural topologies, power levels, energy storage systems, and standards for electric vehicle charging stations and their impacts on grid. *IEEE access*, 9:128069–128094, 2021.

[51] Harold W Kuhn. The hungarian method for the assignment problem. *Naval research logistics quarterly*, 2(1-2):83–97, 1955.

[52] András Frank. On kuhn's hungarian methodâa tribute from hungary. *Naval Research Logistics (NRL)*, 52(1):2–5, 2005.

[53] Rainer E Burkard and Eranda Cela. Linear assignment problems and extensions. In *Handbook of combinatorial optimization: Supplement volume A*, pages 75–149. Springer, 1999.

[54] James Munkres. Algorithms for the assignment and transportation problems. *Journal of the society for industrial and applied mathematics*, 5(1):32–38, 1957.

[55] Christos H Papadimitriou and Kenneth Steiglitz. *Combinatorial optimization: algorithms and complexity*. Courier Corporation, 1998.

[56] G Ayorkor Mills-Tettey, Anthony Stentz, and M Bernardine Dias. The dynamic hungarian algorithm for the assignment problem with changing costs. *Robotics Institute, Pittsburgh, PA, Tech. Rep. CMU-RI-TR-07-27*, 2007.

[57] Huan Liu, Zheng Liu, Shuo Liu, Yihao Liu, Junchi Bin, Fang Shi, and Haobin Dong. A nonlinear regression application via machine learning techniques for geomagnetic data reconstruction processing. *IEEE Transactions on Geoscience and Remote Sensing*, 57(1):128–140, 2018.

[58] Mohsen Shahhosseini, Guiping Hu, and Hieu Pham. Optimizing ensemble weights and hyperparameters of machine learning models for regression problems. *Machine Learning with Applications*, 7:100251, 2022.

[59] Haidara Saleh and Jamil Layous. *Machine Learning -Regression*. PhD thesis, 01 2022.

[60] Yoonsuh Jung. Multiple predicting k-fold cross-validation for model selection. *Journal of Nonparametric Statistics*, 30(1):197–215, 2018.

[61] Oanh Tran Thi Kim, Nguyen H Tran, VanDung Nguyen, Sun Moo Kang, and Choong Seon Hong. Cooperative between v2c and v2v charging: Less range anxiety and more charged evs. In *2018 International Conference on Information Networking (ICOIN)*, pages 679–683. IEEE, 2018.

[62] Christos D Korkas, Simone Baldi, Shuai Yuan, and Elias B Kosmatopoulos. An adaptive learning-based approach for nearly optimal dynamic charging of electric vehicle fleets. *IEEE Transactions on Intelligent Transportation Systems*, 19(7):2066–2075, 2017.

[63] Hayla Nahom Abishu, Abegaz Mohammed Seid, Yasin Habtamu Yacob, Tewodros Ayall, Guolin Sun, and Guisong Liu. Consensus mechanism for blockchain-enabled vehicle-to-vehicle energy trading in the internet of electric vehicles. *IEEE Transactions on Vehicular Technology*, 71(1):946–960, 2021.

[64] Mohamed Baza, Ahmed Sherif, Mohamed MEA Mahmoud, Spiridon Bakiras, Waleed Alasmary, Mohamed Abdallah, and Xiaodong Lin. Privacy-preserving blockchain-based energy trading schemes for electric vehicles. *IEEE Transactions on Vehicular Technology*, 70(9):9369–9384, 2021.

[65] Rabiya Khalid, Muhammad Waseem Malik, Turki Ali Alghamdi, and Nadeem Javaid. A consortium blockchain based energy trading scheme for electric vehicles in smart cities. *Journal of Information Security and Applications*, 63:102998, 2021.

[66] Donghe Li, Qingyu Yang, Dou An, Wei Yu, Xinyu Yang, and Xinwen Fu. On location privacy-preserving online double auction for electric vehicles in microgrids. *IEEE Internet of Things Journal*, 6(4):5902–5915, 2018.

[67] Long Luo, Jingcui Feng, Hongfang Yu, and Gang Sun. Blockchain-enabled two-way auction mechanism for electricity trading in internet of electric vehicles. *IEEE Internet of Things Journal*, 9(11):8105–8118, 2021.

[68] Luyao Zou, Md Shirajum Munir, Yan Kyaw Tun, Seokwon Kang, and Choong Seon Hong. Intelligent ev charging for urban prosumer communities: An auction and multi-agent deep reinforcement learning approach. *IEEE Transactions on Network and Service Management*, 2022.

[69] Mojtaba Abdolmaleki, Neda Masoud, and Yafeng Yin. Vehicle-to-vehicle wireless power transfer: Paving the way toward an electrified transportation system. *Transportation Research Part C: Emerging Technologies*, 103:261–280, 2019.

[70] M Rostami-Shahrbabaki, SA Haghbayan, M Akbarzadeh, and K Bogenberger. On the technical feasibility of vehicle to vehicle charging for electric vehicles via platooning on freeways. In *2022 European Control Conference (ECC)*, pages 530–537. IEEE, 2022.

[71] Samira Hosseini and Abdulsalam Yassine. A novel v2v charging scheme to optimize cost and alleviate range anxiety. In *2022 IEEE Electrical Power and Energy Conference (EPEC)*, pages 354–359. IEEE, 2022.

[72] Kai Liu, Jiangbo Wang, Toshiyuki Yamamoto, and Takayuki Morikawa. Exploring the interactive effects of ambient temperature and vehicle auxiliary loads on electric vehicle energy consumption. *Applied Energy*, 227:324–331, 2018.

[73] Kai Liu, Toshiyuki Yamamoto, and Takayuki Morikawa. Impact of road gradient on energy consumption of electric vehicles. *Transportation Research Part D: Transport and Environment*, 54:74–81, 2017.

[74] Ray Galvin. Energy consumption effects of speed and acceleration in electric vehicles: Laboratory case studies and implications for drivers and policymakers. *Transportation Research Part D: Transport and Environment*, 53:234–248, 2017.

[75] Anastasia Bolovinou, Ioannis Bakas, Angelos Amditis, Francesco Mastrandrea, and Walter Vinciotti. Online prediction of an electric vehicle remaining range based on regression analysis. In *2014 IEEE International Electric Vehicle Conference (IEVC)*, pages 1–8. IEEE, 2014.

[76] Eiman ElGhanam, Mohamed Hassan, and Ahmed Osman. Machine learning-based electric vehicle charging demand prediction using origin-destination data: A uae case study. In *2022 5th International Conference on Communications, Signal Processing, and their Applications (ICCSPA)*, pages 1–6. IEEE, 2022.

[77] Rafael Basso, Balázs Kulcsár, and Ivan Sanchez-Diaz. Electric vehicle routing problem with machine learning for energy prediction. *Transportation Research Part B: Methodological*, 145:24–55, 2021.

[78] Peter Ondruska and Ingmar Posner. Probabilistic attainability maps: Efficiently predicting driver-specific electric vehicle range. In *2014 IEEE Intelligent Vehicles Symposium Proceedings*, pages 1169–1174. IEEE, 2014.

[79] Stephan Rhode, Steven Van Vaerenbergh, and Matthias Pfriem. Power prediction for electric vehicles using online machine learning. *Engineering Applications of Artificial Intelligence*, 87:103278, 2020.

[80] Abdollah Amirkhani, Arman Haghanifar, and Mohammad R Mosavi. Electric vehicles driving range and energy consumption investigation: A comparative study of machine learning techniques. In *2019 5th Iranian Conference on Signal Processing and Intelligent Systems (ICSPIS)*, pages 1–6. IEEE, 2019.

[81] T Rajasekar, Anu Varshini RP, P Mohanraj, K Hemmasri, et al. Reducing driverâs range anxiety for electric vehicle using machine learning. In *2023 8th International Conference on Communication and Electronics Systems (ICCES)*, pages 1251–1257. IEEE, 2023.

[82] Sheng Tian, Chengwei Li, Qing Lv, and Jia Li. Method for predicting the remaining mileage of electric vehicles based on dimension expansion and model fusion. *IET Intelligent Transport Systems*, 16(8):1074–1091, 2022.

[83] Chung-Hong Lee and Chih-Hung Wu. A novel big data modeling method for improving driving range estimation of evs. *IEEE Access*, 3:1980–1993, 2015.

[84] Faten Alenizi and Omer Rana. Minimising delay and energy in online dynamic fog systems. *arXiv preprint arXiv:2012.12745*, 2020.

[85] Plugshare charging station map. Available online: http://www.plugshare.com.

[86] Short-term energy outlook - u.s. energy information administration (eia). Available online: https://www.eia.gov/outlooks/steo/report/electricity.php.

[87] Minimum wage — u.s. department of labor. Available online: view-source:https://www.dol.gov/general/topic/wages/minimumwage.

[88] Energy consumption of full electric vehicles cheatsheet - ev database. Available online: https://ev-database.org/cheatsheet/energy-consumption-electric-car.